

RESEARCH ARTICLE

Long disordered regions of the C-terminal domain of Abelson tyrosine kinase have specific and additive functions in regulation and axon localization

Han S. J. Cheong, Mark F. A. VanBerkum*

Department of Biological Sciences, Wayne State University, Detroit, United States of America

* mvb@wayne.edu



OPEN ACCESS

Citation: Cheong HSJ, VanBerkum MFA (2017) Long disordered regions of the C-terminal domain of Abelson tyrosine kinase have specific and additive functions in regulation and axon localization. PLoS ONE 12(12): e0189338. <https://doi.org/10.1371/journal.pone.0189338>

Editor: Juan-Pablo Labrador, University of Dublin Trinity College, IRELAND

Received: September 29, 2017

Accepted: November 22, 2017

Published: December 12, 2017

Copyright: © 2017 Cheong, VanBerkum. This is an open access article distributed under the terms of the [Creative Commons Attribution License](https://creativecommons.org/licenses/by/4.0/), which permits unrestricted use, distribution, and reproduction in any medium, provided the original author and source are credited.

Data Availability Statement: All relevant data are within the paper and its Supporting Information files.

Funding: This research was supported by a grant from the National Science Foundation (<https://www.nsf.gov/>) (IOS 1121025) to MVB. The funders had no role in study design, data collection and analysis, decision to publish, or preparation of the manuscript.

Competing interests: The authors have declared that no competing interests exist.

Abstract

Abelson tyrosine kinase (Abl) is a key regulator of actin-related morphogenetic processes including axon guidance, where it functions downstream of several guidance receptors. While the long C-terminal domain (CTD) of Abl is required for function, its role is poorly understood. Here, a battery of mutants of *Drosophila* Abl was created that systematically deleted large segments of the CTD from Abl or added them back to the N-terminus alone. The functionality of these Abl transgenes was assessed through rescue of axon guidance defects and adult lethality in *Abl* loss-of-function, as well as through gain-of-function effects in sensitized *slit* or *frazzled* backgrounds that perturb midline guidance in the *Drosophila* embryonic nerve cord. Two regions of the CTD play important and distinct roles, but additive effects for other regions were also detected. The first quarter of the CTD, including a conserved PxxP motif and its surrounding sequence, regulates Abl function while the third quarter localizes Abl to axons. These regions feature long stretches of intrinsically disordered sequence typically found in hub proteins and are associated with diverse protein-protein interactions. Thus, the CTD of Abl appears to use these disordered regions to establish a variety of different signaling complexes required during formation of axon tracts.

Introduction

Abelson tyrosine kinase (Abl) is an essential protein that is a key regulator of cytoskeletal dynamics. Abl is known to aid in the regulation of actin dynamics underlying a myriad of cell processes, ranging from vesicle trafficking and Golgi architecture to cell motility and development [1–4]. Yet, understanding how Abl functions in these cellular processes remains challenging. During development in *Drosophila*, Abl participates in the processes of dorsal closure [5, 6], ventral furrow formation [7], cell adhesion [8, 9], photoreceptor morphogenesis [10, 11], and axon guidance. In particular, Abl has a long-appreciated role in nervous system development, and is thought to be a key link between axon guidance receptors and cytoskeletal activity underlying axon outgrowth and steering.

In this role, Abl functions downstream of a variety of receptors in both repulsive and attractive axon guidance pathways [12–17]. To carry out these functions, Abl cooperates with the adaptor protein Disabled to regulate the actin-associated proteins Enabled (Ena) and Abelson interacting protein (Abi), and further regulates the Rac GTPase through the Trio GEF [18]. Zygotic loss of function of *Abl* causes defects in midline crossing over of axons in the embryonic nerve cord [19] as well as stalling in the ISNb motoneurons at the periphery [20–23]. Indeed, the ladder-like structure of the embryonic nerve cord is severely disrupted if both zygotic and maternal contributions of Abl are removed [5]. To facilitate axon guidance at the midline, Abl is recruited by the Roundabout (Robo) and Frazzled (Fra) receptors, which govern the repulsive (Slit) and attractive (Netrin) pathways respectively. Abl also interacts with the Down Syndrome Cell Adhesion Molecule (Dscam) family of netrin receptors, where it may modulate Robo activity [17, 24, 25]. In the Robo-Slit pathway, Abl is physically recruited by Robo and phosphorylates it, and acts in concert with the actin-binding protein Capulet and microtubule-binding protein Orbit/MAST to regulate the growth cone cytoskeleton [12, 19, 26]. The Netrin receptor Frazzled also recruits Abl, although the precise role of Abl in this pathway is not well understood [13, 15, 27]. Indeed, perturbation of Abl levels in *fra*, *robo* or *slit* mutants cause a variety of axon guidance phenotypes that suggest that the role of Abl in these pathways is mechanistically complex [12–15, 27]. To begin to understand how Abl participates in these processes, several labs have previously focused on examining conserved elements within *Drosophila* Abl.

Initial work clearly documents the presence of both kinase-dependent and -independent functions of Abl in axon guidance and rescue of *Abl* mutant lethality [28]. The identification of significant kinase-independent activity suggests that Abl may function as a scaffold protein, helping form critical signaling complexes during these developmental processes. In this regard, the long CTD of Abl is a primary suspect for a scaffolding role. The possession of a long CTD in Abl family kinases is unique among non-receptor tyrosine kinases, and in *Drosophila* this region of roughly 1100 amino acids is indispensable for Abl function [28]. Comparison of the CTD sequence between vertebrates and invertebrates reveals little amino acid similarity, although all end with an F-actin binding domain (FABD). In vertebrates, this FABD participates in bundling of F-actin [29], localization of Abl to actin filaments [30], and regulation of Abl kinase activity [31, 32]. In *Drosophila*, the FABD is differentially required for axon guidance in various subsets of neurons; it is required for axon guidance of some commissural neurons, but dispensable in ISNb motoneurons [27]. Unique to *Drosophila* Abl are two putative EVH1-binding motifs (F/LPPPP) not present in the vertebrate Abl CTD, that are hypothesized to interact with the actin regulator Enabled (Ena) [33]. In the fly, Ena interacts both physically and genetically with Abl, and is also phosphorylated by Abl to suppress its activity [33–36]. Abl also regulates the subcellular distribution of Ena, and ectopic localization of Ena is a significant contributor to lethality in *Abl* loss-of-function [7, 37]. Thus, the EVH1-binding motifs were expected to be important for the function of Abl.

In an attempt to dissect the role of the CTD, previous work from the Peifer lab identified and examined four regions within the CTD that are conserved between insects (CR1-4) [6]. However, all but one of these regions proved to be dispensable for Abl's function in a variety of actin-related morphogenetic processes. The dispensable regions include CR4, which contains the EVH1-binding motifs. Only deletion of CR1 significantly impairs the function of Abl in dorsal closure and axon guidance. This region contains a single 'canonical' PxxP motif, PAPPKR (a.a. 769–774 in Uniprot accession number# M9PFS1, consensus motifs, R/KxxPxxP or PxxPxR/K, as defined in [38, 39]) that aligns with one of three PxxP motifs in the CTD of vertebrate Abl homologs. In these vertebrate homologs, these three PxxP motifs in the CTD are known to be involved in the recruitment of the adaptor proteins Crk and Nck, as well as the Abelson-interacting (Abi) family of actin-regulating proteins [40–45]. Thus, a similar role

in protein recruitment was hypothesized for the PxxP motif within the CR1 region [6]. Interestingly, several other canonical PxxP motifs exist within the *Drosophila* CTD, although their potential contribution to Abl function remains unknown.

In short, while the long CTD is essential, only small regions exhibit sequence conservation, and even these are not necessarily required for Abl function. So how might the CTD function? Here, we systematically deleted relatively large portions (here termed quarters) of the CTD from Abl and monitored their function. Conversely, we added these selected regions back to the N-terminal region of Abl, to determine which regions are by themselves sufficient to restore function to the kinase-active half of the molecule. Using this strategy, we note additive effects on Abl function throughout the long CTD, as well as two specific functions. We define a new region in the CTD (third quarter, or 3Q) that functions in the recruitment of Abl to axon tracts where it is important for axon guidance. Furthermore, we identify the first quarter (1Q) as a region critical to Abl activity, and while this region contains the previously-identified CR1 region, the conserved PxxP motif, while important, is not the sole contributor to Abl activity within this region. Finally we provide evidence that these regions are characterized by stretches of disorder, likely to function in protein-protein interactions typical of a hub protein. Future work will need to look at these regions in more detail, keeping in mind that specific sequence elements may be less important than overall structure.

Results

The C-terminal domain of *Drosophila* Abl spans ~1100 amino acids (Fig 1A) and is thought to be key for Abl function [28]. Yet those few regions exhibiting significant sequence conservation only play minor roles in Abl function, and the role of the CTD remains poorly understood. Accordingly, we elected to undertake a systematic analysis of the entire C-terminal domain, without relying on any assumptions about the function of any particular stretch. Taking care to avoid disrupting previously identified motifs or domains (Fig 1B), we subdivided the CTD into smaller regions (quarters, or 1-4Q), and systematically deleted these regions of Abl, creating Abl Δ 1Q through Abl Δ 4Q. Conversely, we added these selected regions back to the N-terminal region of Abl (creating N-1Q through N-4Q), to determine which regions are by themselves sufficient to restore function to the kinase-active half of the molecule. Transgenes also include a wild type Abl, as well as constructs expressing only the N-terminal (AblN) or C-terminal (AblCTD) region. All transgenes were inserted via PhiC31-mediated transgenesis into the *ZH-attP-22A* landing site [46] to simplify genetic manipulation and minimize position effects on transgene expression (see S1 Fig for expression data). Having created this battery of Abl mutants, we then tested how manipulation of these CTD regions impacts the ability of our transgenes to rescue *Abl* axon guidance defects and adult lethality.

The first quarter of the Abl C-terminus is critical for Abl function

Zygotic loss of Abl causes ectopic midline crossing errors in the embryonic nerve cord, as quantified in late-stage embryos stained for the axonal marker Fasciclin 2 (mAB 1D4). This antibody labels 3 longitudinal fascicles on each side of the midline within the nerve cord, not crossing the midline when viewed in wild type stage 16/17 embryos (Fig 2). However, in *Abl* zygotic mutants, roughly 50% of embryos show one or more ectopic midline crossovers that are Fas2-positive, a phenotype that serves as the basis for our *Abl* rescue assay. As expected, we can rescue these defects almost fully by pan-neural expression of our wild-type Abl transgene using the *1407-Gal4* driver. When *Abl* transgenes from our CTD deletion series were expressed, transgenes carrying deletions of 3Q or 4Q rescue midline crossover defects to a degree indistinguishable from the wild-type transgene, while deletion of 2Q marginally

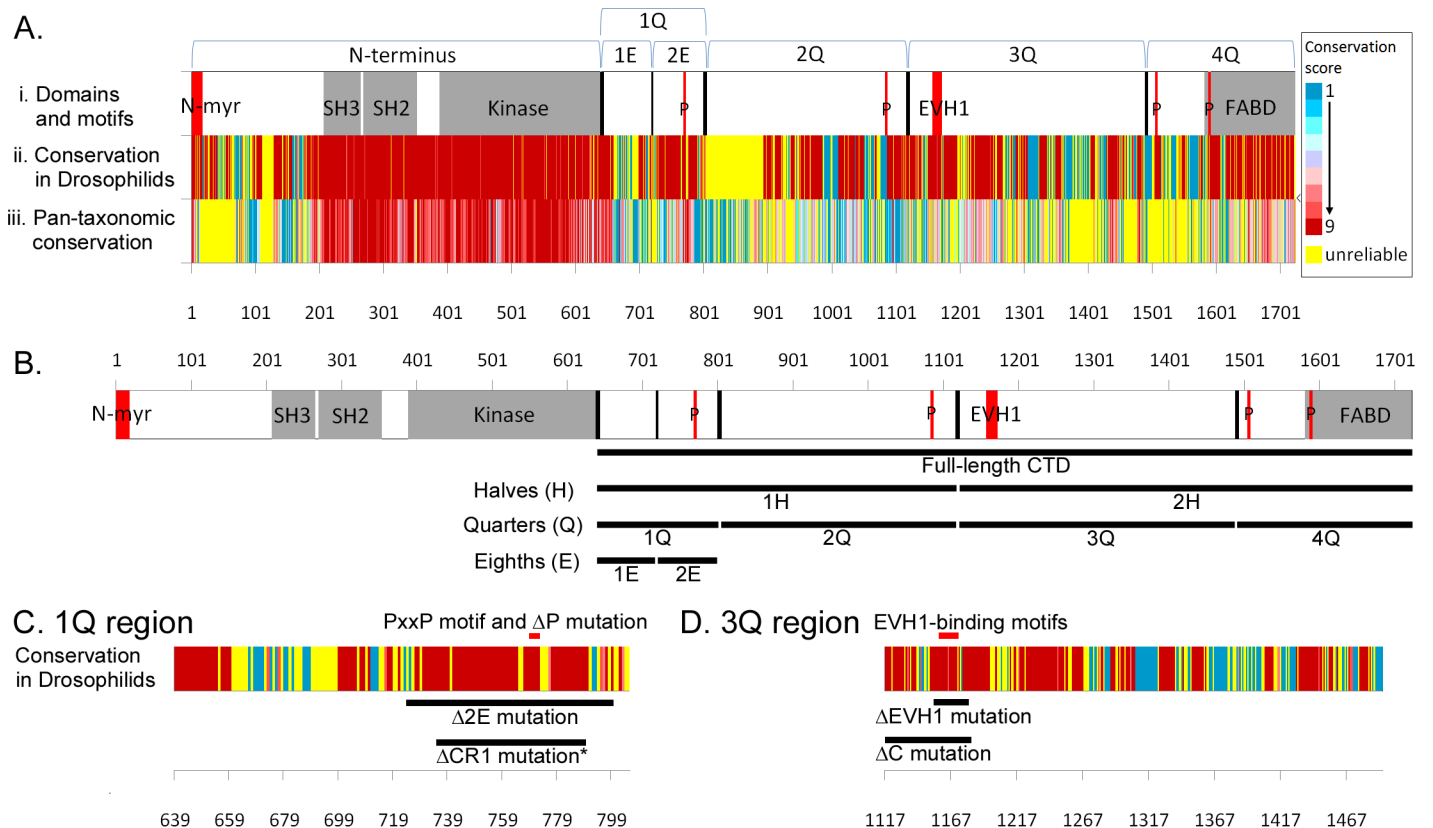


Fig 1. Abl structure and conservation, and CTD mutants made in this study. (A) The *Drosophila* Abl CTD is relatively poorly conserved. (i) Presence of domains annotated by SMART (grey) and motifs (red) in *Drosophila* Abl. Notable motifs are N-terminal myristoylation site (N-myristoylation site), PxxP (P) and EVH1-binding motifs (EVH1). (ii) Conservation of amino acids of Abl in 11 Drosophilid species, as aligned by Clustal Omega and graded using ConSurf. 'Unreliable' conservation scores (yellow) have either less than 6 non-gapped residues in the alignment or a confidence interval of equal to or larger than 4 color grades. (iii) Conservation of amino acids using the same methodology as lane 2, but using 40 Abl homologs from both vertebrates and invertebrates. (B) Line cartoon of *Drosophila* Abl showing the large regions of the CTD (black lines) mutated in this paper. The CTD was divided into halves and quarters. The first quarter was further divided into first and second eighths. All transgenes carry a C-terminal FLAG-tag (not shown). (C) Close-up view of conservation of amino acids in the 1Q region of the Abl CTD, with conservation grade colors as in (A). Also shown are deletions removing the better-conserved second eighth (2E) region, and a comparison to the CR1 deletion as carried out in Rogers et al., 2016 (*). Deletion of the conserved PxxP motif (Δ P) is shown in lane 4. (D) Close-up view of conservation of amino acids in the 3Q region of the Abl CTD. Also shown are a deletion removing the EVH1-binding motifs (Δ EVH1), and a deletion removing a highly conserved region of 3Q that includes EVH1 (Δ C).

<https://doi.org/10.1371/journal.pone.0189338.g001>

impairs rescue (~15% crossovers). Remarkably, the Abl Δ 1Q transgene fails entirely in rescuing these defects (Fig 2C and 2I).

On the other hand, while pan-neural expression of AblN partially rescues some of the ectopic crossovers observed in Abl mutant embryos (~35% embryos with defects), the addition of 1Q, 2Q or 3Q does not significantly improve rescue by AblN, while adding 4Q to AblN abolishes the small amount of rescue seen with AblN alone. Strikingly, rescue is fully restored if both 1Q and 3Q are added to Abl-N, indicating that the 1Q and 3Q regions together provide the majority of the Abl CTD's function in axon guidance at the midline. Together, these data point to a key role for 1Q in axon guidance, although this region alone is not sufficient to restore function to AblN unless 3Q is included.

Rescue of Abl adult lethality

The relative robustness of Abl to removal of individual CTD quarters in the rescue of Abl axon guidance defects was surprising. Thinking that the maternal contribution of Abl [5, 47] may

*Abi*WT, (D) *Abi*N, (E) *Abi*Δ1Q, (F) *Abi*N-1Q, (G) *Abi*ΔP, and (H) *Abi*Δ2E. The *Abi*WT transgene (C) almost fully rescues crossing over defects. *Abi*Δ1Q (E) completely fails to rescue defects while the other transgenes give varying degrees of partial rescue ranging from moderate (*Abi*ΔP) to low (*Abi*N, *Abi*N-1Q). (I) Quantification of crossing over defects. ≥79 embryos were scored over 3 replicates per genotype. Asterisks (*) over a particular column indicate significant difference (p < 0.05) compared to the indicated transgene or genotype. Deletion of 1Q totally abolishes rescue, while the *Abi*N-1Q-3Q transgene is sufficient for rescue at a wild-type level. Mutants that have 1E, 2E or P removed partially impair rescue.

<https://doi.org/10.1371/journal.pone.0189338.g002>

have partially obscured our ability to uncover roles for these regions, we decided to next assess the ability of our mutants to rescue adult lethality. Pupal development is known to represent a significant lethal phase for *Abi* mutants, with only a small number of escapers surviving this step in development [48]. Examination of lethality at this stage likely minimizes the effect of the maternal contribution of *Abi*.

Endogenous *Abi* is widely expressed at low levels in most tissues [49], suggesting that a non-neuronal role for *Abi* might contribute to adult lethality. However, ubiquitous expression with *Act5C-Gal4* produces very few surviving adults (S2A Fig), although some rescue (~15–30%) was provided by *Abi*Δ4Q, *Abi*N-1Q, and *Abi*N-1Q-3Q, all of which lack 4Q while retaining 1Q. As 4Q includes the FABD, these data seem to suggest that the toxic effect of ubiquitously over-expressed *Abi* might be associated with its ability to interact with actin. Given the propensity to cause lethality for most transgenes, we did not pursue rescue with this *Act5C-Gal4* driver line further.

Instead, we focused on the importance of neuronal function of *Abi* in *Abi* adult lethality. Pan-neuronal expression of wild-type *Abi* with *1407-Gal4* rescues about half of the observed lethality in *Abi* mutant flies. Consistent with rescue of axon guidance defects, only removal of 1Q abolishes rescue (Fig 3A), and only the addition of 1Q to the N-terminus restores wild-type

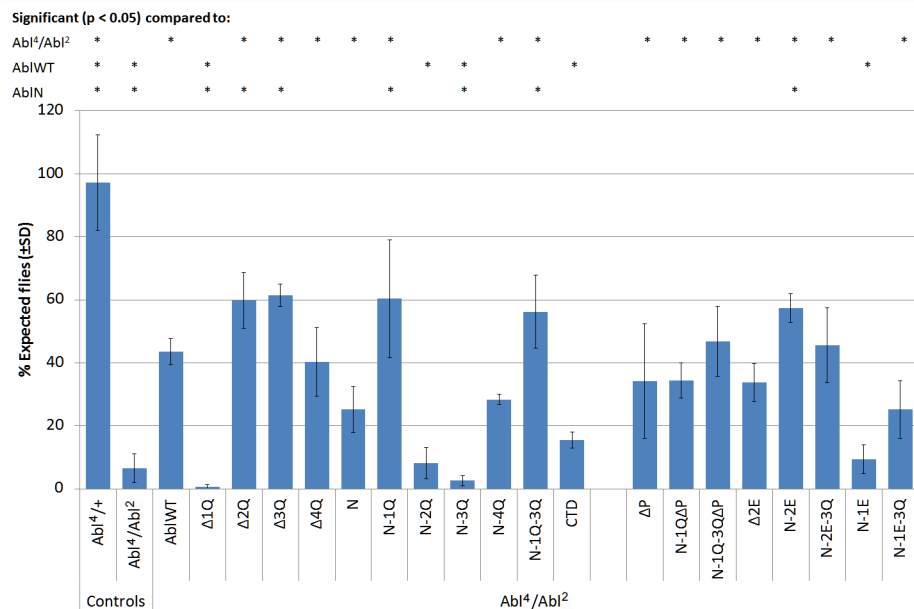


Fig 3. Rescue of adult lethality in homozygous *Abi* mutants by *Abi* transgenes expressed with the 1407-Gal4 driver. Asterisks (*) over a particular column indicate significant difference (p < 0.05) compared to the indicated transgene or genotype. Three replicates of ≥400 flies were counted, with approximately 50 flies for each of males and females in the non-expressing *Abi* heterozygous category. This category was used to normalize rescued *Abi* mutant flies. Deletion of 1Q totally abolishes rescue, while addition of 1Q to *Abi*N gives rescue at the level of the wild-type transgene. Mutants that have 1E, 2E or P removed have small effects on rescue.

<https://doi.org/10.1371/journal.pone.0189338.g003>

viability to AblN.; yet, AblN-1Q is not substantially better than AblN at rescuing axon guidance defects. Similar to rescue of axon guidance defects, AblN-1Q-3Q remains a minimally effective Abl restoring adult viability to the same level as observed for wild type Abl.

It is worth noting that pan-neural expression of the *AblΔ1Q* transgene actually induces lethality in *Abl* heterozygotes (over 60%, S2C Fig). We suspect that this lethality occurs post-embryonic development since the nerve cords of wild type or *Abl* heterozygous embryos still look normal when *AblΔ1Q* is expressed in all neurons. Heterozygous lethality is the first evidence of a gain-of-function effect for the *AblΔ1Q* transgene, suggesting that the transgene may be aberrantly regulated in at least one critical Abl function, or be incorrectly expressed in a subset of neurons.

To address this latter issue, we attempted to better replicate parts of the endogenous Abl expression pattern by using two other *Gal4* lines controlled by *Abl* enhancer fragments, *R60H11* and *R65D01* [50]. Both of these *Abl-Gal4* enhancers drive neuronal expression, although in a smaller subset of neurons and at lower levels than observed with *1407-Gal4* (S3 Fig). For unknown reasons, rescue with these drivers are biased towards adult males, and thus only males are used here for comparison. Considering only males, the rescue observed with both these driver lines is similar in pattern to that observed using the *1407-Gal4* driver, with a couple of notable exceptions (S2B Fig). Most interestingly, the *AblΔ1Q*-dependent lethality observed with *1407-Gal4* is lost using either of the Abl driver lines, suggesting that some cell-specificity or expression level control is important. In addition, *AblN* alone failed to rescue with both Abl drivers even though it partially rescues (30%) with *1407-Gal4*, and a few subtle differences occur as different quarters are added to AblN. A dominant phenotype also emerged using the *60H11* driver, as *Abl* heterozygous flies expressing *AblN*, *AblN-2Q* or *AblN-3Q* fail to carry out wing expansion. This has not been pursued further.

Taken together, it is clear that 1Q plays the largest role in rescue of adult lethality, consistent with rescue of *Abl* axon guidance defects. However, Abl-dependent viability is not always associated with its role in axon guidance (e.g. AblN-1Q), and the removal of 2Q and 4Q regions, which are relatively benign during axon guidance, can subtly alter viability, suggesting that these regions are not simply inert.

Distinct regions of the 1st quarter contribute towards Abl function

The observations that *AblΔ1Q* completely fails to rescue both *Abl* axon guidance defects and adult lethality, while addition of 1Q or 1Q-3Q to AblN results in functional *Abl* transgenes points towards a critical role of the 1Q region for Abl function. By comparative sequence analysis with Abl proteins of other *Drosophila* species, the 1Q region of the Abl CTD can be roughly subdivided into two halves of low and high conservation (1st and 2nd eighths, or 1E and 2E), respectively (Fig 1C). Additionally, the highly conserved half (2E) contains a single canonical PxxP motif (PAPPKR, a.a. 769–774 in Uniprot accession number# M9PFS1) that aligns to a PxxP motif in the CTD of vertebrate Abl homologs. An *Abl* transgene lacking a region roughly equivalent to our 2E region was previously demonstrated to be highly impaired in rescuing Abl-dependent morphogenetic processes [6]. In that work, the PxxP motif was suggested, but not tested, to be the key feature of this region, as PxxP motifs are the minimal consensus motif postulated to be required for interaction with SH3 domains found in certain Abl partners [39, 51, 52].

To specifically test the role of PxxP motif, we created a set of Abl transgenes deleting the PxxP motif (Δ P) in either full length *Abl*, *AblN-1Q* or *Abl-1Q-3Q*. Our rationale for introducing these deletions into *AblN-1Q* and *Abl-1Q-3Q* is based on the observation that the Abl CTD contains 3 other PxxP sequences that fit the canonical type I or type II SH3-binding consensus

motifs [38, 39]; these additional motifs are located in the 2nd and 4th quarters of the CTD (Fig 1A). Recall that the *AblN-1Q* and *AblN-1Q-3Q* transgenes substantially rescued *Abl* loss in our prior *Abl* rescue assays. Therefore, the removal of the 1Q PxxP motif in these minimal transgenes should uncover roles for this particular motif while avoiding any possible redundant contributions from the other PxxP motifs. Along the same lines, we also examined the role of the 1E and 2E regions by deleting them in the same set of transgenes, producing *AblΔ2E*, *AblN-1E*, *AblN-2E*, *AblN-1E-3Q* and *AblN-2E-3Q*.

In terms of axon guidance defects, removal of the PxxP motif reduces, by about half, the ability of full-length *Abl* to rescue these crossover defects, and reduces the rescue of *AblN-1Q-3Q* from near wild-type to the level of *AblN* alone (Fig 2I). This effect is similar but stronger with all transgenes lacking 2E (which contains the PxxP motif), with *AblΔ2E*, *AblN-1E-3Q* and *AblN-1E* rescuing only at the level of *AblN* alone, or worse. Conversely, *AblN-2E-3Q* partially rescued defects, although not at the level of either *AblN-1Q-3Q* or wild-type *Abl*. Clearly the PxxP motif is important for *Abl* function during axon guidance, but the surrounding 2E sequence provides additional function. On the other hand, the severity of the $\Delta 1Q$ mutation cannot be explained either by the loss of the PxxP motif alone or by loss of 2E, and indicates that 2E and its PxxP motif must still cooperate with 1E to provide full wild-type function.

Interestingly, in terms of adult lethality, pan-neural expression of all mutant transgenes, except *AblN-1E* rescues adult lethality indistinguishable from the wild-type transgene (Fig 3); *AblN-1E* only allows a few adults to survive. Curiously, while *AblN-2E-3Q* rescued *Abl* adults to the same level as wild-type *Abl*, it was uniquely the only transgene of this series to cause substantial adult lethality in *Abl* heterozygotes (35% lethality, S2C Fig); this parallels the induced lethality observed with *AblΔ1Q*. Adult rescue using the *1407-Gal4* driver is largely consistent with rescue using the *60H11* and *65D01* *Abl* drivers (S2B Fig), although some minor differences suggest increased sensitivity to the driver's exact expression pattern (or level). We also note that flies expressing *AblN-2E* and *AblN-2E-3Q* with the *60H11* driver fail to expand their wings. This is despite the *AblN-2E* and *AblN-2E-3Q* transgenes rescuing adult lethality at levels close to that observed for the wild-type transgene, showing that they too are slightly impaired in function when 1E is removed (S2B Fig).

In summary, the 2E region and its PxxP motif are the most important region of 1Q, as any transgene that have these motifs removed are impaired in axon guidance. Moreover, transgenes that have 2E deleted (*AblΔ2E*, *AblN-1E* and *AblN-1E-3Q*) do not rescue axon guidance defects as well as their counterparts where only the PxxP motif was removed (*AblΔP*, *AblN-1QΔP* and *AblN-1Q-3QΔP*). These data support our contention that the context of the PxxP motif (i.e. 2E) is important for function, which is consistent with Rogers et al's [6] report on the importance of the equivalent CR1 region. Moreover, as adult rescue appears to be more resistant to removal of these regions, 2E and the PxxP motif may participate only in some of the differential roles of *Abl*, something that future work will have to explore in more detail. Finally, there is some indication that both *AblΔ1Q* and *AblN-2E-3Q* are functional proteins that have gain-of-function effects resulting from the removal of 1E.

Gain-of-function assays reveal further roles for the CTD region

Abl is known to function downstream of numerous guidance receptors during formation of the nerve cord [12–17]. Thus, it was surprising that the 2Q, 3Q and 4Q regions, which together span most of the CTD, are individually dispensable during rescue of *Abl* axon guidance. To further assess the role of the CTD in axon guidance, we turned to an over-expression assay in sensitized genetic backgrounds. Overexpression of *Abl* in a wild-type background only yields a few subtle phenotypes in a small subset of motoneurons [53], yet when over-expressed in

frazzled (fra) homozygous [15] or *slit* heterozygous [14] mutants, leads to gross exacerbation of nerve cord defects. These are dominant phenotypes that occur even with a full complement of maternal and zygotic Abl. Admittedly, we do not yet know much about the molecular mechanisms underlying these defects, but nevertheless, we sought to use the increased sensitivity to Abl signaling to reveal additional contributions of the CTD to Abl function. Indeed, these assays proved to be helpful in identifying contributions of all four quarters during axon guidance.

The repulsive receptor Robo and its ligand Slit are major players in repulsive axon guidance at the *Drosophila* midline, and recruits Abl as one of its downstream effectors [54]. A heterozygous loss of the midline repellent *slit* cause ectopic midline crossovers in the embryonic nerve cord, and the frequency of these increases with over-expression of Abl transgenes [14]. Thus, over-expression of Abl is thought to alter midline repulsion signaling. Here we assessed how our Abl transgenes alter midline guidance by overexpressing them in all neurons of *slit* heterozygous embryos using the *elav-Gal4* driver [14] and scoring ectopic crossovers using mAb 1D4 (Fig 4).

First, we established a baseline level of midline axon guidance defects for the *slit* heterozygous embryos by overexpressing an RFP transgene inserted at the 22A site. About 30% of all *slit* heterozygous embryos exhibit 1 or 2 ectopic crossovers when the RFP control is expressed, and overexpression of wild type Abl doubles these crossovers. Removal of 1Q from Abl severely enhances the midline crossover phenotype (to 100% penetrance), while removal of 3Q

slit² elav-Gal4/+ with UAS transgene

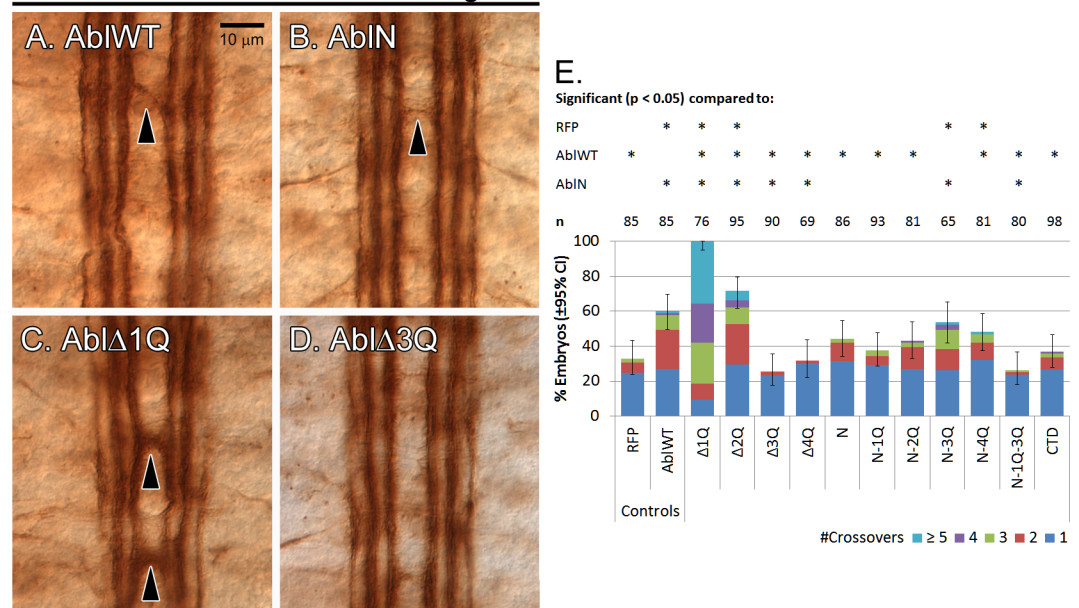


Fig 4. Gain-of-function assay for Abl transgenes in a *slit²* heterozygous background. Abl mutant transgenes were overexpressed pan-neurally in heterozygous *slit²* embryos with the *elav-Gal4* driver, and nerve cords of stage 16–17 embryos were examined for crossing over defects via immunostaining for mAb 1D4. (A–D) Overexpression of transgenes causes midline crossing overs (arrowheads) in a *slit²* heterozygote. Expression of *AblWT* (A) and *AblN* (B) causes moderate crossing over defects. Deletion of 1Q in Abl (C) causes severe crossing over defects, while deletion of 3Q (D) abolishes Abl-induced crossing over defects. (E) Quantification of crossing over defects based on ≥65 embryos per genotype. Asterisks (*) over a particular column indicate significant difference (p < 0.05) compared to the indicated transgene or genotype. *AblΔ1Q* uniquely causes defects in 100% of embryos examined. Of the other transgenes, only *AblΔ2Q*, *AblN-3Q* and *AblN-4Q* cause significantly higher defects than the RFP negative control.

<https://doi.org/10.1371/journal.pone.0189338.g004>

instead suppresses this phenotype back to the baseline level. Interestingly, removal of 4Q also suppresses these Abl-dependent ectopic crossovers, while removal of 2Q mildly enhances the frequency of crossovers over wild-type Abl. The 2Q and 4Q phenotypes are unique to the *slit* assay, and may reflect the selective requirement of these regions during midline repulsive signaling. Of the AblN series, only the addition of 3Q to AblN significantly increases ectopic crossovers to roughly the levels observed with wild-type Abl. On the other hand, even though AblN-1Q-3Q mutant was minimally sufficient to rescue Abl axon guidance defects, it is not capable of inducing ectopic crossovers in the *slit* heterozygote. This points to an interesting interaction between the first and third quarters.

Next we turned to midline attraction using a *frazzled* mutant background. The attractive Netrin receptor Frazzled recruits Abl as a downstream effector [13, 27], although the precise role of Abl in this pathway is not well understood. When wild-type Abl is overexpressed in *fra* homozygous embryos, axon tracts of the nerve cord exhibit many defects, including a loss in posterior commissure formation and an increase in the number of gaps in the longitudinal connectives [15]. In previous work, we had postulated that the development of the ventral cord becomes highly sensitive to Abl signaling levels in the absence of Fra, resulting in numerous defects as Abl presumably began to function incorrectly downstream of other unknown receptors [15]. As such, we anticipated that a *fra* background might be ideal for picking out subtle differences in the function of our Abl transgenes.

We overexpressed our series of transgenes in *fra* homozygotes with *1407-Gal4*, and quantified axon guidance defects in stage 16–17 embryos immunostained with the mAb BP102, which highlights the ladder-like structure of the axon tracts of the embryonic nerve cord (Fig 5). First, we established a baseline for the *fra* homozygous embryos by overexpressing an RFP transgene inserted at the 22A site. At this baseline state, about 40% of embryos exhibit a loss or thinning of posterior commissures, and this almost doubles when the wild-type Abl transgene is overexpressed. A similar trend is seen when gaps in the longitudinal connective are scored. While other guidance defects were also scored (see S1 Table), we focused on the formation of the commissures and longitudinal connectives as Abl has been linked to their development [5, 15, 23, 27].

Unlike wild-type Abl, *AblCTD* alone did not enhance axon guidance defects in *fra* mutants, while AblN had differential effects on commissures and longitudinal connectives. Removal of 2Q had no effect while removal of 4Q slightly increased the number of posterior commissure gaps. Strikingly, deletion of 1Q significantly enhances (to 95%) the severity of posterior commissure gaps, and increases longitudinal defects to 50%, while deletion of 3Q prevents Abl from inducing these defects. Addition of either 1Q or 4Q instead suppresses the ability of AblN to induce defects in *fra* mutants, while differential effects on commissures and longitudinal connectives are seen with the AblN-2Q and AblN-1Q-3Q transgenes. Thus, by using the *fra* background, we uncover evidence indicating that each quarter contributes functionally to Abl as it presumably cooperates with various guidance receptors during formation of commissures or longitudinal connectives.

Given the severity of phenotypes observed when *AblΔ1Q* is overexpressed, we also assessed our series of 1Q mutants in the *fra* background. Surprisingly, deletion of the PxxP motif in wild-type Abl, *AblN-1Q* or *AblN-1Q-3Q* had no effect on the ability of our transgenes to induce defects. Similarly, neither *AblΔ2E* nor *AblN-1E-3Q* was substantially different from their counterparts wild-type Abl and *AblN-1Q-3Q*, respectively. Despite the fact that the comparable *AblN-1Q-3Q* is less effective than wild-type Abl at inducing defects, the *AblN-2E-3Q* transgene caused defects at a higher level (80%) than wild-type Abl, even though it is still capable of partially rescuing both adult lethality and axon guidance defects in our earlier assays. These paradoxical results await further investigation, but do suggest that AblN-2E-3Q may be partially misregulated similar to but not to the same extent as AblΔ1Q.

expression of *RFP* showing baseline level of thinning/gaps in posterior commissures (black arrows) and thinning/gaps in longitudinal connectives (white arrows). *AbiWT* (B) expression causes an increase in defects in posterior commissures and longitudinal connectives, and this is mirrored by *AbiN* (F) and *AbiΔP* (G), while *AbiΔ3Q* (D) and *AbiCTD* (E) have no effect on the *fra* phenotype. Both *AbiΔ1Q* (C) and *AbiN-2E-3Q* (H) cause an increase in defects more severe than *AbiWT*. (I) Quantification of posterior commissure (PC) gaps (I) and longitudinal connectives (LC) gaps (J) in *fra* mutants overexpressing Abl transgenes based on ≥ 55 embryos scored per genotype.

<https://doi.org/10.1371/journal.pone.0189338.g005>

Together the severity of defects in these *fra* mutants reinforce the importance of 1Q in Abl function, and support the premise that this *Abl* transgene is inappropriately regulated. This dysregulation does not appear to be caused by deletion of either the PxxP motif or the 2E region, indicating an involvement of the entire 1Q region in Abl function. Moreover, it is clear that deletion of other quarters also show differential effects on Abl function, especially that of 3Q which suppresses Abl's ability to cause phenotypes in both *slit* and *fra* backgrounds. As described below, this region appears to be important for localization of Abl to axons.

The 3rd quarter of the CTD localizes Abl to axons

During our initial experiments, we assessed the level of Abl transgene expression by immunostaining using the FLAG epitope present at the C-terminus of our transgenes. Wild-type Abl localizes strongly to the axon tracts of the nerve cord, confirming prior reports [27, 28, 49], and localization remained strong even with removal of the EVH1-binding motifs and FABD. Furthermore, while AblN alone localizes poorly to axons, AblCTD is sufficient on its own for strong axonal localization indistinguishable from wild-type Abl (see Fig 6). In support of this, protein produced from the *Abl^l* allele, which introduces a stop codon after the kinase domain, and an Abl transgene substituting the murine Abl CTD for the *Drosophila* CTD, also fail to localize to axons [28]. These data suggest that localization of Abl to axons is a major function of the *Drosophila* Abl CTD, and we set out to define the regions of the CTD responsible for localizing Abl to axons.

First, we generated and expressed a series of transgenes fusing RFP to FLAG-tagged fragments of the Abl CTD and assessed which region(s) was sufficient to localize RFP to axons. The CTD was divided into approximate halves (1-2H) and then quarters (1-4Q, also see Fig 1B). The RFP transgenes were then inserted via PhiC31-mediated transgenesis into the *ZH-attP-86Fb* landing site [46], and expressed in the embryo with *1407-Gal4*. As the intrinsic fluorescence of our RFP transgenic proteins was low, to quantitatively assess the degree of localization of transgenic protein, we carried out fluorescent immunohistochemistry on embryos using anti-FLAG and mAb BP102 antibodies, and took confocal image stacks for at least 3 stage 16–17 embryos per transgene. For each embryo, the area in the flattened confocal stack corresponding to axons in the CNS was defined by the presence of BP102 staining, and the mean intensities within axons and cell bodies determined. The ratio of mean intensity within axons to mean intensity in cell bodies was then taken as a measure of localization.

When expressed in the embryonic nerve cord, only RFP transgenes fused to full-length AblCTD, 2H or 3Q were capable of localizing to axons (Fig 6A–6E). RFP alone localized poorly to axons (axon to cell body ratio of ~ 0.6). Interestingly, quantification of localization showed that while localization of RFP-2H was indistinguishable from the full-length RFP-AblCTD (ratio of ~ 1.5), RFP-3Q localized to axons about half as well (ratio of ~ 1). Thus, both quarters (3Q and 4Q) found in RFP-2H cooperate in axonal localization, although RFP-4Q alone is insufficient. Within the 3Q region, the conserved EVH1-binding motifs are the only recognizable motifs of significant interest. However, localization of 3Q remains intact even if the EVH1-binding motifs are removed (ΔC , also see Fig 1D). Thus, the 3rd quarter, but not the EVH1-binding motifs, is sufficient to direct a heterologous protein to axons.

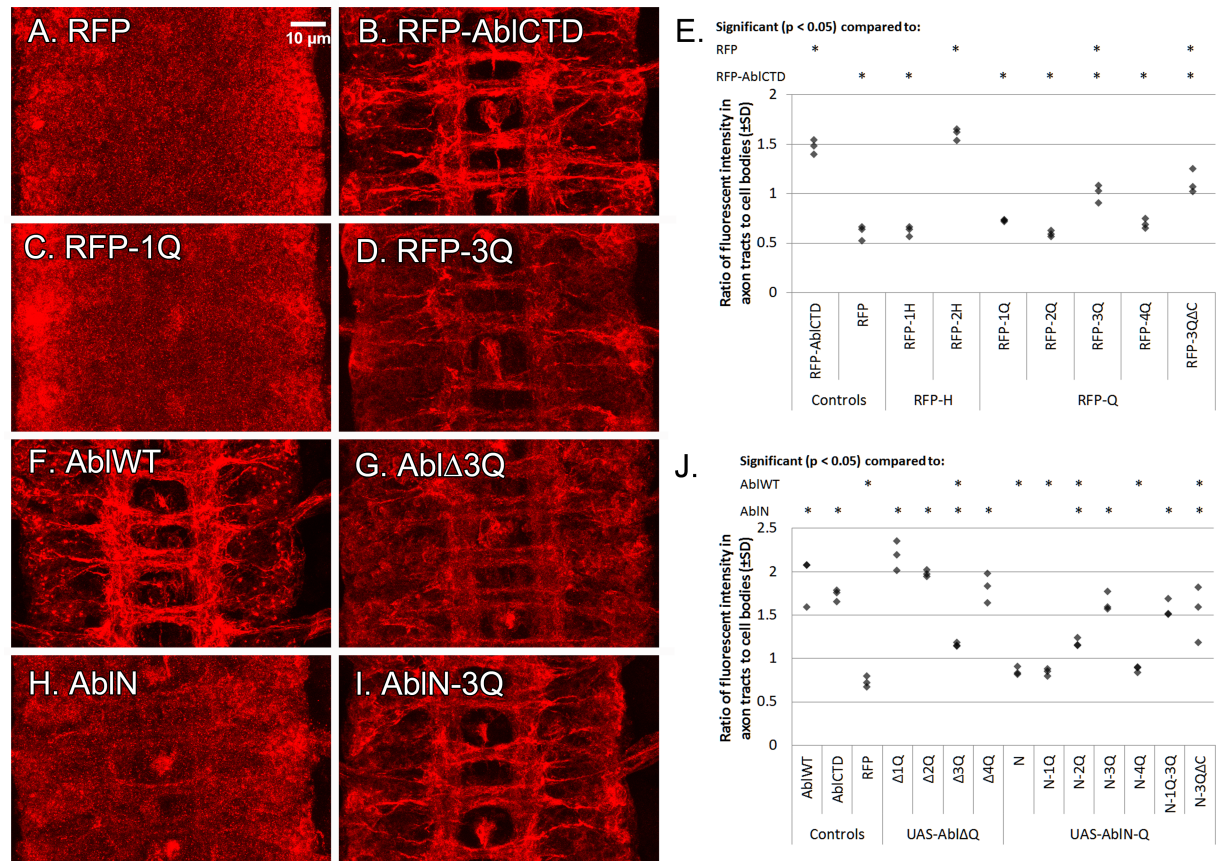


Fig 6. Axonal localization of Abl transgenes. Transgenes were expressed pan-neurally with *1407-Gal4*, and immunostained for the C-terminal FLAG tag. The RFP control (A) is present mainly in cell bodies, while RFP fused to AbICTD (B) localizes strongly to axons. RFP fused to 1Q (C) fails to localize to axons, as do 2Q and 4Q (not shown), but RFP fused to 3Q (D) is localized to axons. (E) Quantification of localization. Areas of axon tracts and cell bodies were defined in flattened confocal stacks for 3 different embryos, and the ratio of fluorescent intensity in axon tracts vs cell bodies was taken as described in Methods. Asterisks (*) over a particular column indicate significant difference ($p < 0.05$) compared to the indicated transgene or genotype. RFP-AbICTD and RFP-2H localize to axons strongly. RFP-3Q localizes to axons less strongly, and removal of a region containing the EVH1-binding motifs (ΔC) does not further change its localization. Full-length Abl (F) localizes strongly to axons, and deletion of 3Q in an Abl transgene (G) reduces this localization. AbIN alone (H) localizes weakly to axons, but addition of 3Q to AbIN (I) significantly restores axonal localization. (J) Quantification of localization, with statistics as in (E). Removal of 3Q, but not 1Q, 2Q or 4Q, from full-length Abl significantly reduces axonal localization. Addition of 3Q in AbIN-3Q and AbIN-1Q-3Q is sufficient to restore near-wildtype localization. Removal of the EVH motifs (ΔC) does not change localization of AbIN-3Q.

<https://doi.org/10.1371/journal.pone.0189338.g006>

Next, we sought to test the significance of each quarter in the context of full-length Abl using our set of mutant Abl transgenes (Fig 6F–6J). In embryos, both full-length Abl and AbICTD were enriched in the axon tracts of the nerve cord as expected (ratio of ~1.8), while very little AbIN is localized to axons (ratio of 0.8). Deletion of 1Q, 2Q or 4Q had no noticeable impact on localization of the protein. On the other hand, deletion of 3Q significantly impaired axonal localization (ratio of 1.15) compared to the wild-type Abl protein, but did not fully abolish it as compared to AbIN alone (ratio of 0.8). Furthermore, addition of 3Q to AbIN, but not any other quarter, resulted in significant restoration of axonal localization (ratio of 1.65). This localization remains intact even if the EVH1-binding motifs are removed from the 3Q region (ΔC).

Thus, the 3Q region of the Abl CTD is sufficient for localization by itself to axon tracts, and is partially required for localization in the context of full-length Abl. The ability to recruit Abl

to axons where it is required for axon guidance is consistent with the ability of the AblN-1Q-3Q transgene to rescue *Abl* guidance defects despite the inability of AblN-1Q to do so. Impaired localization may also explain the observation that Abl Δ 3Q induces fewer axon guidance phenotypes in the *slit* and *fra* backgrounds, as well as the increased ability of AblN-3Q to cause defects in these genetic backgrounds.

The 1st and 3rd quarters of the AbICTD are disordered

The Abl CTD, including the 1Q and 3Q regions, is largely devoid of known or putative protein domains, except for the C-terminal FABD (Fig 1A). As such, it is not immediately obvious how 1Q and 3Q carry out their roles in Abl function and localization. To gain some insight, we undertook an extensive bioinformatic analysis of the CTD sequence using available online tools including SMART [55], CDD[56], JPred [57], and ELM [58]. Of these, the IUPred and ANCHOR prediction tools [59–62] suggested that the majority of the CTD, including 1Q and 3Q, is not only disordered, but may become ordered upon binding to other proteins (Fig 7A), thereby providing a mechanism where these regions could participate in protein-protein interactions. Accordingly, we set out to verify that these regions are indeed disordered using a protease sensitivity assay [63]. The principle of this assay is based on the observation that disordered regions are highly flexible and solvent-exposed, and are thus far more sensitive to proteolytic cleavage compared to globular regions. This selective susceptibility is easily demonstrated through partial proteolysis of the protein with carefully-titrated concentrations of protease.

To obtain a substrate for digestion, we fused the 1Q and 3Q regions to an N-terminal GST tag and retained a FLAG-tag on the C-terminus. For technical reasons, neither the full-length Abl protein nor the full-length Abl CTD could be bacterially expressed. Recombinant protein was expressed in *E. coli* and purified on glutathione agarose. Importantly, the globular GST domain of these recombinant proteins serves as an internal control in our protease sensitivity assay, as it is expected to be more resistant to cleavage compared to the putative disordered regions. The protease clostripain (Endoproteinase Arg-C), was chosen for this assay, as a similar number of cleavage sites are present in both GST and the 1Q and 3Q regions (10 in GST, 8 in 1Q, and 12 in 3Q; Fig 7B). Using both GST-1Q and -3Q, we titrated a range of protease concentrations that yielded a range of partial digest fragments.

The susceptibility of the 1Q and 3Q regions to digestion is readily observed using anti-FLAG and anti-GST western blots. The anti-FLAG immunoblots (Fig 7C and 7D) indicate that digestion at lower concentrations produce only a single digested FLAG-tagged fragment for GST-1Q, and a series of fragments for GST-3Q. The sizes of these digested fragments are consistent with the utilization of cut sites within the 1Q and 3Q regions, and not within the GST domain. Conversely, anti-GST immunoblotting reveals a series of GST-tagged fragments for both digests with sizes ranging between that of the full-length GST-1Q or 3Q, and GST alone, again consistent with the utilization of cut sites only within the CTD fragments. To further demonstrate the resistance of the GST domain relative to 1Q and 3Q, we carried out a more complete digestion with high protease concentrations (10x and 100x, as indicated on Fig 7C and 7D). At these concentrations, FLAG-tagged fragments are quickly lost, while a GST-tagged band remains at the expected size for the entire GST domain alone (28 kD) that only begins to show slight digestion at the highest protease concentration. Total protein stains for these digests do not reveal additional major bands (S4 Fig).

Using recombinant protein, the above assay demonstrated that the 1Q and 3Q regions, at least, are likely to be disordered. But is disorder also a hallmark of Abelson itself? As we could not isolate recombinant full length Abl from bacteria, we established lysates from third instar

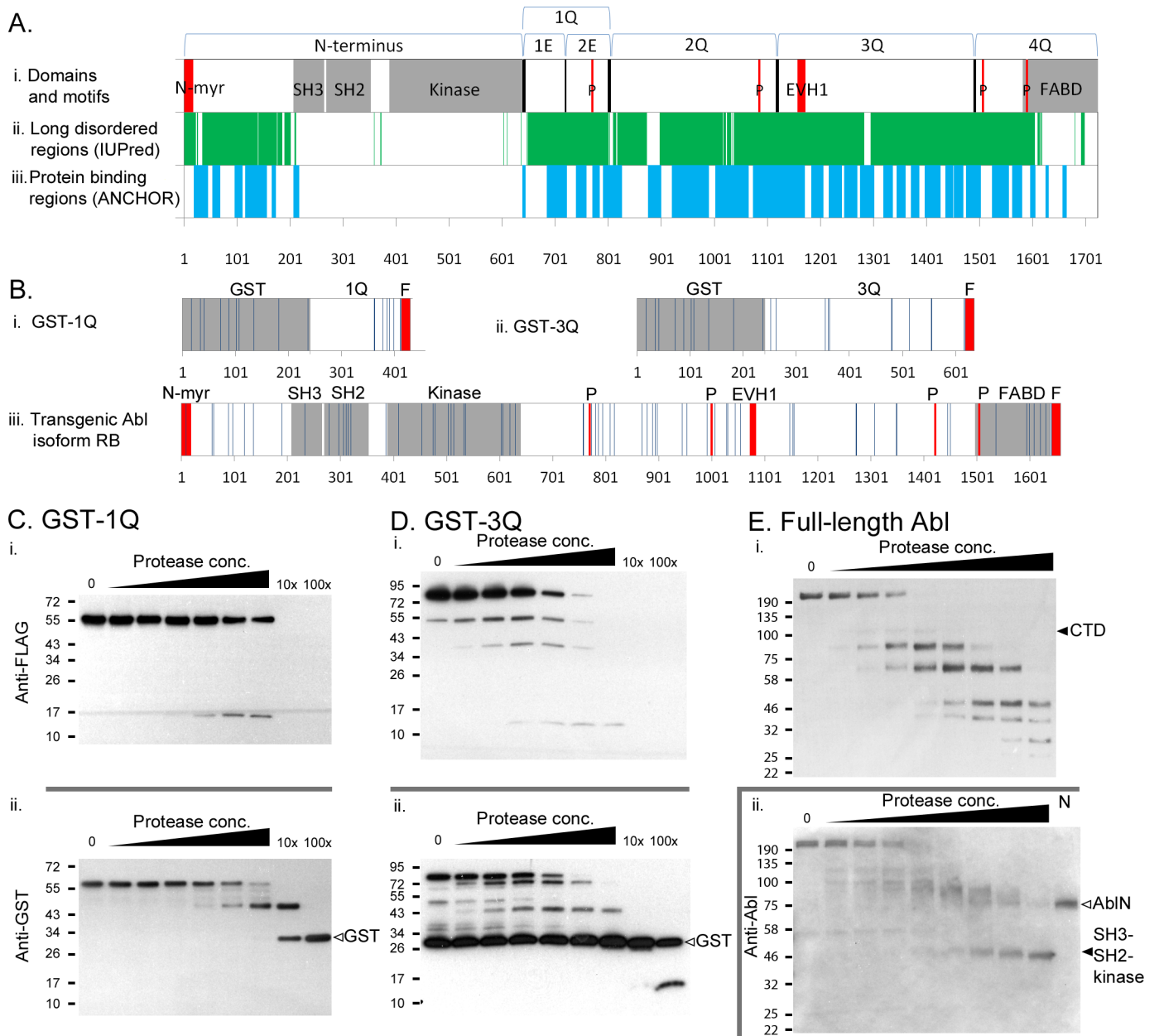


Fig 7. Protease susceptibility assay reveals disorder in the Abl CTD. (A) Predicted intrinsic disorder (IUPred) and protein binding regions (ANCHOR) within Abl. (B) Predicted clostripain (endoproteinase Arg-C) digestion sites within GST-1Q, GST-3Q and full-length Abl for protease susceptibility assay. Sites are well distributed over both the globular domains and predicted disordered regions, and sites within disordered regions should be preferentially utilized. Clostripain digest of purified GST-1Q (C) and GST-3Q (D) with 6 lanes of increasing doses, and two final lanes with 10x and 100x protease as indicated. All FLAG-tagged fragments are more than ~25kD smaller than the full-length protein, and no GST-tagged fragments are smaller than the ~25kD GST domain (▷) except at the 100x protease concentration for GST-3Q. Both indicate that protease sites within the CTD fragments are preferentially utilized by clostripain, compared to the GST domain. (E) Clostripain digest of full-length transgenic Abl in total cell lysates of 3rd instar CNS. FLAG-tagged fragments are present at the size of the full-length CTD (~108 kD) or smaller, consistent with preferential digestion within the CTD. Fragments labeled with a polyclonal antibody against the Abl N-terminus show either fragments at or above the size of full-length AblN (~69 kD, ▷) or at the size of the SH3-SH2-domain (~49 kD, ▷). In the last lane, AblN (N) alone was also expressed in 3rd instar CNS, but the lysate was not subject to digestion.

<https://doi.org/10.1371/journal.pone.0189338.g007>

CNS pan-neurally expressing FLAG-tagged Abl. These lysates contain reasonable quantities of full length, as noted when we confirmed expression of our transgenes (see S1 Fig). Lysates

were digested for 30 minutes at room temperature with clostripain, which has many predicted cut sites in both the globular (SH3-SH2-Kinase) domains as well as the CTD (Fig 7B). Given the use of a total lysate, the excess protein helps ensure limited digestion of Abl, and Abl digestion products could still be selectively examined by western blotting using either an anti-FLAG antibody that recognizes the C-terminal FLAG tag, or an anti-Abl antibody [64] recognizing the N-terminus including the globular SH3-SH2-kinase domain cassette. Immunoblotting with either antibody reveals that even under lysate conditions, digestion with clostripain yields a wide range of fragments consistent with disordered regions. That is, all FLAG-tagged fragments are at or below the expected size for the full-length CTD, indicating that their corresponding cut sites were within the CTD, rather than the Abl N-terminus. Conversely, immunoblotting with anti-Abl showed a series of fragments with sizes between full-length Abl and Abl N-terminus alone (69 kD), again consistent with utilization of cut sites primarily within the CTD. At higher protease concentration, a lower ~49kDa band appears that is consistent with the size of the SH3-SH2-kinase domain cassette. It is likely that the N-cap has been digested at these concentrations, and interestingly, the ANCHOR tool also predicts this region to be disordered (Fig 7A). In further support of this, the N-cap region was not resolved in the vertebrate Abl crystal structure, indicating likely disorder [65].

Together, digestion patterns with GST-1Q, 3Q and full-length Abl are consistent with high levels of disorder within the Abl CTD. Future work will have to evaluate whether they also participate in partner binding, as would be predicted based on several other studies of disordered regions [66–68].

Discussion

In the three decades following Henkemeyer et al’s [28] first demonstration of the CTD’s indispensability, remarkably little headway has been made towards the understanding of the contribution of the C-terminal domain to *Drosophila* Abl function. In contrast to previous studies, we evaluated the functions of the entire length of the CTD by systematically removing large regions, to assess how this affects Abl function in axon guidance and viability. Surprisingly, Abl activity largely withstands the removal of these quarters, with the exception of the first quarter, which is absolutely essential (Fig 8). Conversely, no individual quarter (including the first) fully restores function to the N-terminus. A minimally functional Abl requires both the first and the third quarter (Abl-N-1Q-3Q), consistent with the importance of the first quarter in Abl activity and the third quarter in axon localization. However, we also uncovered subtle roles for both 2Q and 4Q in our axon guidance assays. For example, while removing 2Q mostly had no effect on Abl activity in our *Abl* rescue assays, its removal enhances midline crossover defects in a *slit* mutant, and addition of 2Q onto AblN allows it to increase the frequency of

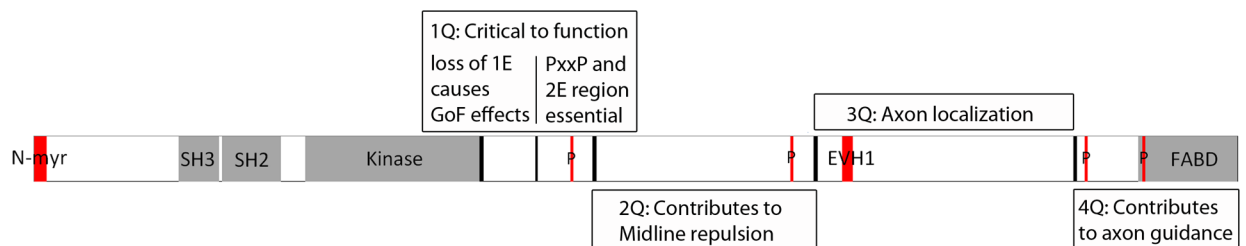


Fig 8. Summary schematic highlighting the role of each region of the CTD. A linear model of Abl is depicted with each quarter of the CTD delineated. The accompanying text boxes provide short statements highlighting the role that each region is thought to contribute to Abl function, as determined in our analysis. See text for details. GoF: gain-of-function.

<https://doi.org/10.1371/journal.pone.0189338.g008>

posterior commissure gaps, but not longitudinal gaps, in a *fra* mutant. Both of these results suggest that 2Q contributes specifically to midline repulsive signaling.

Similarly, 4Q also has a complex effect on Abl activity. Addition of 4Q to AblN inhibits the small amount of *Abl* axon guidance rescue seen with AblN alone, and suppresses the frequency of defects observed in *fra* mutants. Surprisingly, AblN-4Q did not alter AblN function in a *slit* mutant, although the removal of 4Q prevents ectopic crossovers in a *slit* mutant, and enhances commissure loss in a *fra* mutant. As the predominant feature of 4Q is the FABD, we hypothesize that mutations of 4Q have subtly altered the ability of Abl to regulate actin dynamics in response to receptor activation. In other work, the FABD has been linked to regulation of Abl kinase activity [31], and removal of the FABD resulted in *Abl* transgenes that were largely functional, but were subtly impaired in specific morphogenetic and midline axon guidance functions, especially when kinase activity of Abl was also removed [6, 27].

Clearly, the whole CTD contributes to Abl function, in a complex manner, likely involving different protein-protein interactions. We hypothesize that these roles are expedited by the large stretches of intrinsically disordered structure in the CTD biochemically validated in our protease assays. These disordered regions are further predicted to become ordered by gaining stabilizing energy through protein-protein interactions [61]. Importantly, large spans of disorder is predicted in the CTD of both vertebrate and invertebrate Abl (see also S5 Fig) and therefore likely conserved across evolutionary history. Thus, we posit that despite divergence of primary sequence during evolution, the main function of the Abl CTD is that of a scaffolding role, much of which may be mediated by these disordered regions.

The first quarter (1Q) plays a key regulatory role

Of our defined CTD regions, the first quarter of the CTD (1Q) is clearly the most critical region for Abl function and cannot be removed without adversely impairing function of the protein. We suspect that *Abl*Δ1Q is not simply a functional null, as it also displays the most severe axon guidance phenotypes in our *fra* and *slit* gain-of-function assays, and causes significant lethality (60%) in *Abl* heterozygous animals. However, while returning 1Q by itself to AblN is sufficient to rescue adult lethality, it is relatively benign in terms of axon guidance; *AblN-1Q* fails to rescue axon guidance defects in *Abl* mutants, and does not induce gain-of-function phenotypes in *fra* or *slit* mutants. Indeed, 1Q and 3Q are minimally required together for full rescue of axon guidance, while also exhibiting few phenotypes in gain-of-function assays. The 1Q region contains a conserved sequence region, CR1 (roughly equivalent to our 2E region), previously documented by Rogers et al. [6] to reduce Abl function in many actin morphogenic events when deleted, but gain-of-function effects for this mutant were not reported. These authors postulated that the PxxP motif within CR1 carries out the key function of this region, likely through interaction of binding partners such as Crk, Nck and Abi identified in vertebrate work [40–45].

Here, we explicitly tested the role of the PxxP motif in 1Q, and also assessed whether other PxxP motifs found in 2Q and 4Q could act redundantly. Significantly, the PxxP deletion (ΔP) is the smallest mutation we made that impacts Abl function in axon guidance, and it does so in the full-length *Abl* as well as in the minimal *AblN-1Q-3Q* transgene, which lacks all other PxxP motifs. Clearly, the PxxP motif in 1Q carries out an essential function that cannot be fully replaced by the other PxxP motifs. However, the sequence context of the PxxP motif is also important. If the PxxP motif carries out the main function of 1Q, then we predict that ΔPxxP, Δ2E, and Δ1Q should impair Abl function to the same degree. Yet, *Abl*ΔP retains more activity than *Abl*Δ2E in axon guidance rescue, and neither of these deletions replicate the severe gain-of-function effects observed when the entire 1Q is deleted. These data further suggests that, while 2E and its PxxP motif are the most important regions of 1Q, 1E must also contribute to

Abl function in some contexts. This conclusion is perhaps best highlighted by the observation that the *AblN-2E-3Q* transgene, which does not have 1E, induces lethality in heterozygous animals, a feature shared only with *AblΔ1Q*.

Significantly, although the sequence of the 2E region is conserved when considering *Drosophila*, no obvious conservation is evident between this region and the equivalent region around the PxxP motif in vertebrate Abl (Fig 1A). On the other hand, we note the presence of disorder around the PxxP motifs of both vertebrate and *Drosophila* Abl (Fig 7A and S5 Fig), and these regions have at least one common binding partner, Abi [43, 44, 69]. This suggests that conservation of this disorder may be functionally important. In other proteins, the structural plasticity of disordered regions allow them to aid in binding to partners via an induced fit mechanism [70], similar to how adjacent amino acids in other interaction motifs help determine the specificity of binding partners. Along this line it is worth pointing out that the 1E regions is also characterized by stretches of disorder, suggesting disorder may be generally important to the function of 1Q.

The relative importance of 1Q in Abl function raises the possibility that 1Q plays a major role in regulating the scaffolding function of the entire CTD. The Crk and Nck partners identified in vertebrate work [40–42, 45] are themselves scaffold or adaptor proteins, and their recruitment through 1Q may aid in directing protein recruitment in the rest of the CTD, thus changing the output of Abl. Similarly, binding of Abi to 1Q likely recruits the SCAR/Wave complex to Abl [71, 72], and almost certainly serves as an important link between Abl and actin dynamics. It is even conceivable that these interactions regulate Abl kinase indirectly—binding of both Abi [43, 69] and Crk family proteins [73, 74] have been shown to activate Abl kinase activity. More significantly, binding of these different partners to the same PxxP motif necessitates that these interactions be mutually exclusive. Which of these interactions are most important for Abl's role in axon guidance, as examined in our work, needs to be delineated in future studies before potential roles in regulation of Abl kinase activity become worth pursuing. Clearly, the protein-protein interactions mediated by 1Q and their effects on the scaffolding and regulatory interactions mediated by the rest of the CTD will be worth exploring.

Axon localization

Previous work established the importance of localizing Abl to axons [27, 28, 49]. Here, we show that 3Q is the only region that is sufficient to localize a heterologous protein (RFP) to axons and is the major, although probably not sole, determinant of axon localization of Abl itself. Consistent with the role of 3Q in localization, we find that it is important for the rescue of axon guidance defects in *Abl* mutants (e.g. *AblN-1Q-3Q* vs *AblN-1Q*) and in generating gain-of-function phenotypes in *fra* or *slit* mutants (e.g. *Abl-N-3Q*).

Presently, the exact subcellular localization of Abl within the axon is unknown as we cannot distinguish between localization to the cell cortex, microtubules or axoplasm. Both RFP and *AblN* alone have a weak presence in axons, which we suspect represents primarily diffusion, although in the case of *AblN* a contribution from the SH3-SH2 domains might reinforce this localization. The axonal enrichment of Abl when 3Q is present is then likely to be due to an active process that could involve recruitment to membrane complexes, or transport down an axon in association with transport machinery and cytoskeletal elements. In epithelial cells, Abl localizes to the apical cortex, where it aids in actin morphogenic events that may involve Disabled and Ena [7, 64, 75]. However, as we could remove the EVH1 motifs within 3Q without altering axon localization, Ena binding alone is not likely to recruit 3Q to axons. We further note that RFP-2H, containing both 3Q and 4Q, localizes RFP to axons stronger than 3Q alone. Given the presence of the FABD in 4Q, we hypothesize that localization activity mediated

primarily by 3Q might be stabilized by FABD-dependent interactions with actin. As the remaining regions of 3Q are characterized by intrinsic disorder, we hypothesize that axon localization is likely to be mediated by protein-protein interactions involving these disordered regions. This idea will be tested in future proteomic work.

Intrinsic disorder and Abl function: Is Abl a hub protein?

The Abl CTD is highly susceptible to limited protease digestion, a hallmark of intrinsically disordered regions. Disordered regions are now being recognized as a major feature of 'hub' proteins such as BRCA1 [76], p53 [70], and myc [77, 78], all of which, like Abl, participate in diverse cellular processes. Intrinsically disordered regions provide structural plasticity ideal for participation in a variety of protein-protein interactions, including multiple simultaneous interactions or a series of individual interactions, perhaps via small linear motif elements dispersed throughout the CTD [66–68]. Certainly, the sheer size of the CTD, with most of the ~1100 amino acids predicted to be disordered, provides considerable opportunity for a diverse set of interactions. For example, in the case of p53, a major hub protein associated with dozens of targets, just over two-thirds of its protein interactions are mediated by the disordered N- and C-terminal regions [70]. In some cases, competition between binding partners for a particular interface is observed, a phenomenon that may be occurring in the 2E region if the disorder surrounding the PxxP motif helps dictate binding partners (Crk, Nck or Abi). On the other hand, p53 also appears to use larger stretches of disorder to bind to several partners simultaneously [70]. In this case, the various disordered regions of the Abl CTD would be expected to display a level of promiscuity, binding to many partners to form dynamic, heterogeneous 'fuzzy' complexes [79]. This could in part explain why our deletion transgenes often display differential effects between the *Abl*, *fra* and *slit* genetic backgrounds, especially with regard to the subtle additive effects observed for 2Q mutants in our *slit* and *fra* gain-of-function assays.

In conclusion, given the parallels to p53, we propose that Abl functions as a hub protein, using the intrinsic disorder of its CTD to participate in a variety of protein-protein interactions underlying Abl's myriad of cell functions. Minimally, if it is indeed disorder, rather than specific sequences, which is conserved in the CTD, and govern function, future examination of Abl will have to move away from a focus on single motifs and towards identifying protein partners participating in signaling or scaffolding mediated by larger regions of the CTD.

Materials & methods

Bioinformatics

Amino acid sequences for Abl homologs were retrieved from the Ensembl and EnsemblGenomes databases [80, 81] (see S2 and S3 Tables for full set of homologs used in alignment). Multiple sequence alignments were carried out via Clustal Omega [82, 83], and the evolutionary conservation of amino acid sequences were estimated using the ConSurf web server in sequence-only mode [84–87]. Protein domains in Abl homologs were annotated using SMART [88, 89], and motifs and other features were manually annotated. Intrinsic disorder predictions were carried out using the IUPred web server for long disorder prediction [59, 90], and predictions of protein binding regions within disordered regions were carried out using the ANCHOR web server [61, 62].

Fly genetics and stocks

Flies were cultured at 25°C on standard cornmeal-molasses medium on a 12 hour light/dark cycle. The following alleles were used: *Abl*⁴, *Abl*², *fra*⁴, *fra*³, *slit*², *Su(P)*^{EY13245}, and UAS-

mCD8-GFP. The following Gal4 drivers were used: *insc*^{Mz1407} (*1407-Gal4*), *Act5C-Gal4*, *elav-Gal4*, *65D01-Gal4*, and *60H11-Gal4*. *UAS-Abl* transgene stocks are as further described below. Stocks were balanced over LacZ-containing balancer chromosomes where appropriate for detection of embryo genotypes. Other fly stocks were obtained from Bloomington Drosophila Stock Center.

Transgenic constructs

For Abl transgenes with deletions of 1Q, 2Q, 3Q, 4Q or ΔP, Δ1E and Δ2E mutations, Abl cDNA was subcloned from a pMT vector [14] into the pUASTattB vector [46] for PhiC31-mediated transgenesis. Deletions of CTD quarters in this construct were then carried out via PCR site-directed mutagenesis, with the insertion of an AgeI site at the joints. The ΔP, Δ1E and Δ2E mutations were made via the Phusion site-directed mutagenesis method with blunt end-joining. For transgenes containing Abl CTD fragments joined to either RFP or AblN, RFP and AblN constructs were first made in the pUASTattB vector, containing either BsrGI/NotI or AgeI/NotI sites at their C-termini for insertion of CTD fragments. Fragments were then amplified with the appropriate sites and inserted. The AblN-1Q transgene was amplified as a single fragment from the 5' end of the Abl N-terminus to the end of the 1Q region, then inserted into the pUASTattB vector. Primer sequences are found in S4 Table.

Transgenic constructs containing multiple deletions were carried out either via multiple rounds of site-directed mutagenesis, or by assembly of fragments from constructs containing single deletions. All constructs were verified by sequencing. Transgenic flies were generated by germline transformation into fly stocks containing the *M{vas-int.Dm}ZH-2A* maternal integrase source and an attP landing site. The *ZH-attP-86Fb* landing site was used for RFP transgenes, while the *ZH-attP-22A* landing site was used for Abl transgenes [46]. All fly germline transformations were carried out by Rainbow Transgenic Flies, Inc.

Expression levels of Abl transgenes were compared by dissecting 5 CNS's from 3rd instar larvae expressing said transgenes with *1407-Gal4*, following by lysis in SDS sample buffer. Anti-FLAG western blots were carried out with 1:10000 monoclonal rat anti-FLAG L5 (Thermo Fisher, Cat# MA1-142-1MG, Lot# QB215988) followed by 1:20000 polyclonal HRP-conjugated Goat anti-rat antibody (Jackson ImmunoResearch, Cat# 112-035-003). Blots were then reprobed with 1:500 monoclonal mouse anti-β-tubulin (DSHB, Cat#E7, Lot# 1/30/14) followed by 1:20000 polyclonal HRP-conjugated goat anti-mouse antibody (Jackson Immuno-tech, Cat# 115-035-003, Lot# 120344). Dissections and western blots were repeated 3 times.

Embryo collection, immunohistochemistry, and immunofluorescence

Embryos were collected by standard techniques as previously detailed [14]. Briefly, flies were allowed to mate and lay embryos overnight on apple juice agar. Embryos were collected and dechorionated with 25% bleach, then fixed in formaldehyde-saturated heptane for 45 min. Vitelline membranes were cracked by addition of methanol to embryos in heptane followed by vigorous shaking and further washes in methanol, then rehydrated in PBT (1x PBS, 0.1% Triton X-100). To mark embryos carrying LacZ balancer chromosomes, embryos were then incubated in X-gal staining solution (1x PBS, 2 mM MgCl₂, 5 mM potassium ferrocyanide, 5 mM potassium ferricyanide, 4 μL/mL 20% X-gal in dimethylformamide) for 1–3 hours. Embryos were then post-fixed in 4% formaldehyde in PBS for 10 min.

For immunohistochemistry, embryos were incubated with either monoclonal antibody 1D4 (DSHB, Cat# 1D4 anti-Fas II-s, Lot# 12/3/09) or BP102 (DSHB, Cat# BP 102 anti-CNS axons-s, Lot# 07/Apr/10) at a 1:10 dilution in PBT + 5% normal goat serum for 4 hours or overnight. Secondary polyclonal HRP-conjugated goat anti-mouse antibody (Jackson

Immunotech, Cat# 115-035-003, Lot# 120344) was used at a 1:500 dilution with incubation for 4 hours or overnight. Chromogenic detection was carried out by incubation of embryos in Stable DAB solution (Thermo Fisher, Cat# 750118) for a few minutes until appropriately intense staining was observed. Embryos were then washed with PBT and cleared in 70% glycerol. Imaging was carried out on a Leica DM5500 B microscope with differential interference contrast optics and a HCX PL APO 100x/1.40–0.70 OIL objective at room temperature. Images were captured with a Leica DFC425C color camera using the LAS AF acquisition software.

For immunofluorescence to determine localization of transgenic Abl proteins, devitelled embryos fixed in formaldehyde-saturated heptane were not subject to X-gal staining but were used directly for staining. Embryos were incubated overnight for each of the following antibodies, with washes with PBT between antibodies: 3:2000 monoclonal rat anti-FLAG L5 (Thermo Fisher, Cat# MA1-142-1MG, Lot# QB215988), 3:1000 polyclonal Dylight 594-conjugated goat anti-rat (Thermo Fisher, Cat# SA5-10020, Lot# RF2218502), 1:5 mAb BP102 (DSHB, Cat# BP 102 anti-CNS axons-s, Lot# 07/Apr/10), 3:2000 polyclonal Alexa 488-conjugated Goat anti-mouse (Jackson Immunosciences, Cat# 115-545-166, Lot# 128727). Embryos were then counterstained with 1 µg/mL DAPI dihydrochloride in PBS (Santa Cruz Biotechnology, Cat# sc-3598) for 20 minutes, and then cleared in 90% glycerol.

Embryonic phenotype quantification

Embryos were sorted by developmental stages as previously defined [91], and were counted by a trained scorer blinded to embryo genotypes. Scoring was done on a Leica DM5500B microscope at 1000x magnification with brightfield and differential interference contrast optics.

For rescue of *Abl* midline crossover defects and enhancement of *slit* midline crossover defects, whole mount embryos of stages 16–17, stained for mAb 1D4 were analyzed. All abdominal and thoracic segments were evaluated for each embryo. Ectopic crossing overs were defined as Fas2-positive axon bundles crossing the midline and joining the Fas2-positive fascicles on the opposite side. Three replicates per genotype were counted, with about 30 embryos per replicate.

For analysis of guidance defects in *fra* mutants, whole mount embryos of stages 15–17 stained for mAb BP102 were analyzed. All abdominal and thoracic segments were evaluated for each embryo. Commissures were analyzed on a per-segment basis, while longitudinal connectives were analyzed at the intersegmental region. Thinning of commissures or longitudinal connectives was defined as a moderate but visible reduction in thickness of BP102-positive axons in that region, while gaps were defined as a complete or near-complete loss of BP102-positive axons.

Imaging and quantification of Abl localization

For quantification of Abl localization, embryonic nerve cords of filleted stage 17 embryos were mounted in Vectashield antifade reagent (Vector labs, Cat#H-1000) and imaged using the Leica TCS SP5 point scanning confocal system attached to the Leica DMI6000 CS inverted microscope at room temperature using a HC PL APO 100x/1.44 OIL CORR CS objective, with the LAS X image acquisition software. Images were acquired as a confocal stack with 0.3 µm slices such as to span the vertical width of the axon tracts of the nerve cord. Confocal microscopy was done at the Microscopy, Imaging and Cytometry Resources Core at Wayne State University, School of Medicine. Quantification of localization was done using the Fiji software [92, 93]. To distinguish between areas of axon tracts and cell bodies, stacks were flattened, and any area outside the nerve cord was first manually excluded from analysis. Fluorescent signal in the green channel, stained for the BP102 axonal marker, was thresholded using the

minimum cross entropy method [94] built into Fiji. The thresholded channel was then used as a mask to select the area corresponding to axon tracts in the red anti-FLAG channel, while the inverse selection of this area was defined as the cell bodies. The mean intensity of FLAG staining was measured in these two areas, and background levels of fluorescence were subtracted using equivalent measurements from the average of 3 non-expressing embryos. The ratio of intensity in axon tracts vs cell bodies were taken as a measure of Abl localization. Measurements were taken for 3 replicate nerve cords per transgene.

Adult lethality counts

In scoring rescue, it is important to establish a category of flies from the same cross that allows us to determine the number of progeny we might expect if fully rescued. This category of progeny consists of flies that are expected to fully eclose at a wild-type rate, and we use *Abl* heterozygous flies that do not express any transgene for this purpose. For *Abl* adult lethality rescue using UAS-*Abl* transgenes, the following schemes were used. For the *Act5C-Gal4* and 3rd chromosome *Abl-Gal4* lines, R60H11 and R65D01 [50], *UAS-Abl; Abl² e/TM3, Sb Act-LacZ* females were crossed to *Gal4 Abl⁴/+* males. The R60H11 and R65D01 drivers were selected out of a larger collection of *Abl-Gal4* lines constructed with various *Abl* enhancer fragments, based on their relatively widespread expression in a large subset of CNS neurons (see S3 Fig for expression patterns). Rescued *Abl* homozygous flies (*w; UAS-Abl/+; Gal4 Abl⁴/Abl² e*) were normalized to non-expressing, *Abl²* heterozygous flies (*w; UAS-Abl/+; Abl² e/+*). Three replicates of ~200 flies each were counted.

For rescue with the *1407-Gal4* driver, the following scheme was used:

$$y w; UAS-Abl; Abl^2/TM3, Sb Act-LacZ \times y w; 1407-Gal4/+; Abl^4/Su(P)^{EY13245}$$

The *Su(P)^{EY13245}* allele is a homozygous viable P-element insertion adjacent to the *Abl* gene, that carries both mini-white and mini-yellow markers. The mini-yellow marker allows us to distinguish *Abl* heterozygous flies (*Abl²/Su(P)^{EY13245}*) from *Abl* homozygous flies. Flies carrying the *1407-Gal4* insertion were further distinguished by intensity of the mini-white eye color. Rescued flies (*y w; 1407-Gal4/UAS-Abl; Abl⁴/Abl²*) were normalized to *Abl* heterozygous flies not expressing the transgene (*y w; UAS-Abl/+; Abl²/Su(P)^{EY13245}*). Three replicates of ~400 flies each were counted.

GST constructs and E. coli expression

The pGEX-6P-1 vector was modified by site-directed mutagenesis to include AgeI and PmeI sites in the multicloning site. 1Q and 3Q were cloned as a FLAG-tagged AgeI/PmeI fragment into said vector. GST-1Q and 3Q were expressed in the *E. coli* BL21 strain at 18°C, and purified on Glutathione Sepharose 4B (GE Life Science, Cat#17075601) and eluted with reduced glutathione. Excess glutathione was dialyzed before further use.

Protease susceptibility assay

Digestion was carried out in digestion buffer consisting of 50 mM Tris pH 7.4, 150 mM NaCl, 1 mM CaCl₂, 1 mM 2-mercaptoethanol and 1% IGEPAL-CA630 (Sigma-Aldrich, Cat# I8896). For digestion of GST-1Q and -3Q, a range of 6 clostripain (Worthington Biochemical Corporation, Cat# LS001641) concentrations ranging from 2×10^{-1} to 6.25×10^{-3} µg/mL (doubling dilutions) was set up in 100 µL volume of digestion buffer. Clostripain concentrations of 0, 2 (10x) and 20 (100x) µg/mL were also set up. Following that, ~5 µg purified GST-1Q or -3Q in 20 µL buffer was added to each digest, and digestion was carried out for 30 min at room

temperature. Digests were stopped with 2x SDS loading buffer containing 5 mM EDTA and 1mM PMSF, followed by 5 minutes incubation at 95°C. Anti-FLAG western blots were carried out with 1:10000 monoclonal rat anti-FLAG L5 (Thermo Fisher, Cat# MA1-142-1MG, Lot# QB215988) followed by 1:20000 HRP-conjugated polyclonal Goat anti-rat antibody (Jackson ImmunoResearch, Cat# 112-035-003). Anti-GST western blots were carried out with 1:5000 polyclonal rabbit anti-GST (FisherSci, Cat# CAB4169, Lot# QJ210646) followed by 1:10000 polyclonal HRP-conjugated Goat anti-rabbit antibody (Jackson ImmunoResearch, Cat# 111-035-144). Digestions were repeated 3 times.

For digestion of full-length Abl, the wild-type *UAS-Abl* transgene was expressed in 3rd instar larvae with *1407-Gal4*. The CNS of 10 third instars were dissected, pooled and frozen. CNSes were lysed in 200 μ L of 50 mM Tris pH 7.4, 150 mM NaCl, 1% IGEPAL-CA630, 0.5x ProBlock Gold Protease Inhibitor Cocktail (Gold Biotechnology, Cat# GB-108-2), 1 mM EDTA by 20 strokes of a Dounce homogenize with pestle B. Lysate was cleared by centrifugation, and was used immediately for clostripain digestion. A range of 8 clostripain concentrations ranging from 2 to 1.563×10^{-3} μ g/mL (doubling dilutions), as well as a zero control, were set up in 100 μ L volumes. 20 μ L lysate was added to each digest, and digestions were carried out as for GST-1Q and -3Q. Anti-FLAG western blots were carried out as for GST-1Q and -3Q. Anti-Abl western blots were carried out with 1:5000 polyclonal rabbit anti-Abl [64] (a kind gift from Dr. Edward Giniger) followed by 1:10000 polyclonal HRP-conjugated Goat anti-rabbit antibody (Jackson ImmunoResearch, Cat# 111-035-144). Digestions were repeated 3 times.

Statistical analyses

All statistical analyses were carried out in R version 3.3.1 with the multcomp [95], MASS [96], ggplot2 [97], car [98], and DHARMA [99] packages.

For axon guidance defect counts in embryos in the *Abl*, *fra* or *slit* genetic backgrounds, data from all 3 replicates for each separate dataset (*Abl*, *fra* or *slit*) were pooled and fitted to negative binomial generalized linear models, with number of defects per embryo as the response variable and transgene expressed as the predictor variable. Appropriateness of the negative binomial distribution over the poisson distribution was determined using the dispersion test [100–102] to estimate overdispersion. Scaled residual plots were produced using the DHARMA package for diagnostics, and examined manually.

For adult lethality counts normalized rescued fly counts were transformed by the square root transformation. Homogeneity of variances of the transformed values was determined by Levene's test from the car package, and data was then fitted to an ANOVA model with the square root of normalized rescued fly counts as the response variable and transgene expressed as the predictor variable. Diagnostic plots were produced using the ggplot2 package, and manually examined. Post-hoc analysis was carried out with Dunnett's test from the multcomp package, and comparisons were made between the entire transgene set and the *Abl^A/Abl^L*, *AblWT*, and *AblN* treatments.

For quantification of Abl transgenic protein localization, ratios of axon to cell body intensity were transformed by the \log_{10} transformation to fit assumptions of normality. Homogeneity of variances of the transformed values was determined by Bartlett's test [103], and data was then fitted to a one-way ANOVA model with \log_{10} ratio of axon to cell body intensity as the response variable and transgene expressed as the predictor variable. Diagnostic plots were plotted with R utilizing the ggplot2 package, and examined manually. Post-hoc analysis was carried out with Dunnett's test from the multcomp package. For the Abl transgene dataset, comparisons were made between the entire transgene set and the AblN and AblWT transgenes

individually. For the RFP transgene dataset, comparisons were made between the entire transgene set and the RFP and RFP-AblCTD transgenes, individually.

Supporting information

S1 Fig. Expression levels of *Abl* transgenes generated in this work. Transgenes were expressing in 3rd instar CNS's with *1407-Gal4*, and 5 CNS's were dissected and lysed in SDS sample buffer. Western blots shown are representative of three replicates.

(TIF)

S2 Fig. Adult rescue by Abl CTD mutant transgenes. Asterisks (*) over a particular column indicate significant difference ($p < 0.05$) compared to *Abl*¹/*Abl*² homozygous embryos. (A) *Abl* transgenes were ubiquitously expressed using the *Actin5C-Gal4* driver and the percent of expected adults eclosing of either sex is quantified. Three replicates of approximately 200 flies were counted, with at least 50 flies in the non-expressing *Abl* heterozygous category. Only *Abl* Δ 4Q, *AblN*-1Q, *AblN*-1Q-3Q and *AblCTD* show significant rescue. Mutants that have 1E, 2E or P removed have small effects on rescue. (B) Quantification of *Abl*¹/+ heterozygote survival when *Abl* transgenes are pan-neurally expressed with *1407-Gal4*. These counts are from the same dataset as Fig 3A. Only *Abl* Δ 1Q and *AblN*-2E-3Q cause significant lethality compared to non-expressing *Abl* heterozygotes in this condition. (C) Rescue for males with the *1407-Gal4*, *65D01-Gal4* and *60H11-Gal4* drivers. For the *65D01-Gal4* and *60H11-Gal4* drivers, three replicates of approximately 200 flies were counted, with approximately 50 flies in the non-expressing *Abl* heterozygous category, used to normalize rescued *Abl* mutant flies. Only males are shown for comparison purposes as the *65D01-Gal4* and *60H11-Gal4* drivers give poor rescue for females. Significance indicated by symbols as defined in legend top right corner.

(TIF)

S3 Fig. Expression pattern of the *1407-Gal4*, *65D01-Gal4* and *60H11-Gal4* drivers in embryos and larval CNS. The indicated drivers were used to express *UAS-mCD8-GFP*, and embryos/larvae were immunostained for GFP. Stage 13/17 whole mount embryos and 3rd instar larval CNS are shown for *1407-Gal4* (A), *65D01-Gal4* (B) and *60H11-Gal4* (C).

(TIF)

S4 Fig. Total protein stain for clostripain digests of GST-1Q (A) and -3Q (B). Digests from Fig 7 were stained for the total protein stain Sypro Ruby. The symbols \triangleright GST-1Q and \triangleright GST-1Q indicate expected sizes for full-length protein. \blacktriangleright C indicates expected bands originating from added clostripain.

(TIF)

S5 Fig. Bioinformatic analysis of two representative vertebrate Abl homologs. The following sections apply to both murine ABL1 (A) and ABL2/ARG (B): (i) Presence of domains as annotated by SMART (grey) and motifs (red). Nuclear localization and export signals, and additional functional regions are as previously defined [104–108]: high mobility group 1-like boxes (HLB, in pink), F-actin binding region (FAB, in teal) and microtubule-binding region (MT, in purple). (ii) The CTD of both murine ABL1 and ABL2/ARG are intrinsically disordered as predicted by IUPred. (iii) Both CTDs have disordered regions that may function in protein binding as predicted by ANCHOR.

(TIF)

S1 Table. Quantification of various axon guidance defects caused by overexpression of *Abl* transgenes in a *fra* homozygous background. Shown here are per-embryo defect counts for anterior commissure thinning and gaps, posterior commissure thinning and longitudinal

connective thinning. Posterior commissure gaps and longitudinal connective gaps are shown in Fig 5.

(PDF)

S2 Table. Gene names and Uniprot accession numbers of Drosophilid *Abl* homologs used for multiple sequence alignment.

(PDF)

S3 Table. Gene names and Uniprot accession numbers of vertebrate and invertebrate *Abl* homologs used for multiple sequence alignment.

(PDF)

S4 Table. Primers used in the generation of *Abl* mutant transgenes in this work.

(PDF)

Acknowledgments

We appreciate the work of several undergraduate students who assisted in lining up embryos for analysis, including Jessica C. Love, Lana Mirza, Alexandra Petroj, Adeel Siddiqui, and Mariam Zunnu Rain, as well as David Pierce for his technical assistance. Dr. Russell Finley kindly shared the pUASTattB vector used for transgenesis, and Dr. Edward Giniger kindly shared the Abl N-terminus antibody. We are also grateful to Dr. Victoria Meller for advice on our lethality analysis, Dr. Grant Bowman for discussions about hub proteins, and Dr. Athar Ansari for discussions about limited protease digestions. Drs. Carl Freeman and Alexander Gow were very helpful in overseeing our statistical analysis. The Microscopy, Imaging and Cytometry Resources Core is supported, in part, by NIH Center grant P30 CA022453 to the Karmanos Cancer Institute at Wayne State University, and the Perinatology Research Branch of the National Institutes of Child Health and Development at Wayne State University. The BP102 and 1D4 monoclonal antibodies developed by Dr. Corey Goodman, and E7 monoclonal antibody developed by Dr. Michael Klymkowsky, were obtained from the Developmental Studies Hybridoma Bank, created by the NICHD of the NIH and maintained at The University of Iowa, Department of Biology, Iowa City, IA 52242. Stocks obtained from the Bloomington Drosophila Stock Center (NIH P40OD018537) were used in this study. This research was supported by a grant from the National Science Foundation (IOS 1121025) to MVB.

Author Contributions

Conceptualization: Han S. J. Cheong, Mark F. A. VanBerkum.

Data curation: Han S. J. Cheong.

Formal analysis: Han S. J. Cheong, Mark F. A. VanBerkum.

Funding acquisition: Mark F. A. VanBerkum.

Investigation: Han S. J. Cheong, Mark F. A. VanBerkum.

Methodology: Han S. J. Cheong.

Project administration: Mark F. A. VanBerkum.

Resources: Mark F. A. VanBerkum.

Supervision: Mark F. A. VanBerkum.

Visualization: Mark F. A. VanBerkum.

Writing – original draft: Han S. J. Cheong, Mark F. A. VanBerkum.

Writing – review & editing: Han S. J. Cheong, Mark F. A. VanBerkum.

References

1. Kannan R, Giniger E. New perspectives on the roles of Abl tyrosine kinase in axon patterning. *Fly* (Austin). 2017;0. <https://doi.org/10.1080/19336934.2017.1327106> PMID: 28481649.
2. Wang JY. The capable ABL: what is its biological function? *Mol Cell Biol*. 2014; 34(7):1188–97. <https://doi.org/10.1128/MCB.01454-13> PMID: 24421390; PubMed Central PMCID: PMC393570.
3. Colicelli J. ABL tyrosine kinases: evolution of function, regulation, and specificity. *Sci Signal*. 2010;3(139):re6. <https://doi.org/10.1126/scisignal.3139re6> PMID: 20841568; PubMed Central PMCID: PMC2954126.
4. Lanier LM, Gertler FB. From Abl to actin: Abl tyrosine kinase and associated proteins in growth cone motility. *Current opinion in neurobiology*. 2000; 10(1):80–7. PMID: 10679439.
5. Grevengoed EE, Loureiro JJ, Jesse TL, Peifer M. Abelson kinase regulates epithelial morphogenesis in *Drosophila*. *The Journal of cell biology*. 2001; 155(7):1185–98. <https://doi.org/10.1083/jcb.200105102> PMID: 11756472; PubMed Central PMCID: PMC2199330.
6. Rogers EM, Spracklen AJ, Bilancia CG, Sumigray KD, Allred SC, Nowotarski SH, et al. Abelson kinase acts as a robust, multifunctional scaffold in regulating embryonic morphogenesis. *Mol Biol Cell*. 2016; 27(16):2613–31. <https://doi.org/10.1091/mbc.E16-05-0292> PMID: 27385341; PubMed Central PMCID: PMC4985262.
7. Fox DT, Peifer M. Abelson kinase (Abl) and RhoGEF2 regulate actin organization during cell constriction in *Drosophila*. *Development*. 2007; 134(3):567–78. <https://doi.org/10.1242/dev.02748> PMID: 17202187.
8. Tamada M, Farrell DL, Zallen JA. Abl regulates planar polarized junctional dynamics through beta-catenin tyrosine phosphorylation. *Developmental cell*. 2012; 22(2):309–19. <https://doi.org/10.1016/j.devcel.2011.12.025> PMID: 22340496; PubMed Central PMCID: PMC3327890.
9. Zulueta-Coarasa T, Tamada M, Lee EJ, Fernandez-Gonzalez R. Automated multidimensional image analysis reveals a role for Abl in embryonic wound repair. *Development*. 2014; 141(14):2901–11. <https://doi.org/10.1242/dev.106898> PMID: 24948602.
10. Xiong WJ, Rebay I. Abelson Tyrosine Kinase Is Required for *Drosophila* Photoreceptor Morphogenesis and Retinal Epithelial Patterning. *Dev Dynam*. 2011; 240(7):1745–55. <https://doi.org/10.1002/dvdy.22674> WOS:000292155800011. PMID: 21674685
11. Xiong W, Morillo SA, Rebay I. The Abelson tyrosine kinase regulates Notch endocytosis and signaling to maintain neuronal cell fate in *Drosophila* photoreceptors. *Development*. 2013; 140(1):176–84. <https://doi.org/10.1242/dev.088799> PMID: 23175629; PubMed Central PMCID: PMC3513998.
12. Bashaw GJ, Kidd T, Murray D, Pawson T, Goodman CS. Repulsive axon guidance: Abelson and Enabled play opposing roles downstream of the roundabout receptor. *Cell*. 2000; 101(7):703–15. PMID: 10892742.
13. Forsthoefel DJ, Liebl EC, Kolodziej PA, Seeger MA. The Abelson tyrosine kinase, the Trio GEF and Enabled interact with the Netrin receptor Frazzled in *Drosophila*. *Development*. 2005; 132(8):1983–94. <https://doi.org/10.1242/dev.01736> PMID: 15790972.
14. Hsouna A, Kim YS, VanBerkum MF. Abelson tyrosine kinase is required to transduce midline repulsive cues. *J Neurobiol*. 2003; 57(1):15–30. <https://doi.org/10.1002/neu.10232> PMID: 12973825.
15. Dorsten JN, Varughese BE, Karmo S, Seeger MA, VanBerkum MF. *PloS one*. 2010; 5(3):e9822. <https://doi.org/10.1371/journal.pone.0009822> PMID: 20352105; PubMed Central PMCID: PMC2843715.
16. Moresco EM, Koleske AJ. Regulation of neuronal morphogenesis and synaptic function by Abl family kinases. *Current opinion in neurobiology*. 2003; 13(5):535–44. PMID: 14630215.
17. Andrews GL, Tanglao S, Farmer WT, Morin S, Brotman S, Berberoglu MA, et al. Dscam guides embryonic axons by Netrin-dependent and -independent functions. *Development*. 2008; 135(23):3839–48. <https://doi.org/10.1242/dev.023739> PMID: 18948420; PubMed Central PMCID: PMC2712571.
18. Kannan R, Song JK, Karpova T, Clarke A, Shivalkar M, Wang B, et al. The Abl pathway bifurcates to balance Enabled and Rac signaling in axon patterning in *Drosophila*. *Development*. 2017; 144(3):487–98. <https://doi.org/10.1242/dev.143776> PMID: 28087633; PubMed Central PMCID: PMC5341800.
19. Wills Z, Emerson M, Rusch J, Bikoff J, Baum B, Perrimon N, et al. A *Drosophila* homolog of cyclase-associated proteins collaborates with the Abl tyrosine kinase to control midline axon pathfinding. *Neuron*. 2002; 36(4):611–22. PMID: 12441051.

20. Wills Z, Marr L, Zinn K, Goodman CS, Van Vactor D. Profilin and the Abl tyrosine kinase are required for motor axon outgrowth in the *Drosophila* embryo. *Neuron*. 1999; 22(2):291–9. PMID: [10069335](#).
21. Crouner D, Le Gall M, Gates MA, Giniger E. Notch steers *Drosophila* ISNb motor axons by regulating the Abl signaling pathway. *Curr Biol*. 2003; 13(11):967–72. PMID: [12781136](#).
22. Giniger E. A role for Abl in Notch signaling. *Neuron*. 1998; 20(4):667–81. PMID: [9581760](#).
23. Kuzina I, Song JK, Giniger E. How Notch establishes longitudinal axon connections between successive segments of the *Drosophila* CNS. *Development*. 2011; 138(9):1839–49. WOS:000289406900018. <https://doi.org/10.1242/dev.062471> PMID: [21447553](#)
24. Sterne GR, Kim JH, Ye B. Dysregulated Dscam levels act through Abelson tyrosine kinase to enlarge presynaptic arbors. *Elife*. 2015;4. ARTN e05196 <https://doi.org/10.7554/eLife.05196> WOS:000374263000001. PMID: [25988807](#)
25. Alavi M, Song MM, King GLA, Gillis T, Propst R, Lamanuzzi M, et al. Dscam1 Forms a Complex with Robo1 and the N-Terminal Fragment of Slit to Promote the Growth of Longitudinal Axons. *PLoS biology*. 2016;14(9). ARTN e1002560 <https://doi.org/10.1371/journal.pbio.1002560> WOS:000386128900016. PMID: [27654876](#)
26. Lee H, Engel U, Rusch J, Scherrer S, Sheard K, Van Vactor D. The microtubule plus end tracking protein Orbit/MAST/CLASP acts downstream of the tyrosine kinase Abl in mediating axon guidance. *Neuron*. 2004; 42(6):913–26. <https://doi.org/10.1016/j.neuron.2004.05.020> PMID: [15207236](#).
27. O'Donnell MP, Bashaw GJ. Distinct functional domains of the Abelson tyrosine kinase control axon guidance responses to Netrin and Slit to regulate the assembly of neural circuits. *Development*. 2013; 140(13):2724–33. <https://doi.org/10.1242/dev.093831> PMID: [23720041](#); PubMed Central PMCID: PMC3678342.
28. Henkemeyer M, West SR, Gertler FB, Hoffmann FM. A novel tyrosine kinase-independent function of *Drosophila* abl correlates with proper subcellular localization. *Cell*. 1990; 63(5):949–60. PMID: [2175256](#).
29. Van Etten RA, Jackson PK, Baltimore D, Sanders MC, Matsudaira PT, Janmey PA. The COOH terminus of the c-Abl tyrosine kinase contains distinct F- and G-actin binding domains with bundling activity. *The Journal of cell biology*. 1994; 124(3):325–40. PMID: [8294516](#); PubMed Central PMCID: PMCPMC2119935.
30. Hantschel O, Wiesner S, Guttler T, Mackereth CD, Rix LL, Mikes Z, et al. Structural basis for the cytoskeletal association of Bcr-Abl/c-Abl. *Mol Cell*. 2005; 19(4):461–73. <https://doi.org/10.1016/j.molcel.2005.06.030> PMID: [16109371](#).
31. Woodring PJ, Hunter T, Wang JY. Inhibition of c-Abl tyrosine kinase activity by filamentous actin. *The Journal of biological chemistry*. 2001; 276(29):27104–10. <https://doi.org/10.1074/jbc.M100559200> PMID: [11309382](#).
32. Woodring PJ, Litwack ED, O'Leary DD, Lucero GR, Wang JY, Hunter T. Modulation of the F-actin cytoskeleton by c-Abl tyrosine kinase in cell spreading and neurite extension. *The Journal of cell biology*. 2002; 156(5):879–92. <https://doi.org/10.1083/jcb.200110014> PMID: [11864995](#); PubMed Central PMCID: PMC2173320.
33. Niebuhr K, Ebel F, Frank R, Reinhard M, Domann E, Carl UD, et al. A novel proline-rich motif present in ActA of *Listeria monocytogenes* and cytoskeletal proteins is the ligand for the EVH1 domain, a protein module present in the Ena/VASP family. *EMBO J*. 1997; 16(17):5433–44. <https://doi.org/10.1093/emboj/16.17.5433> PMID: [9312002](#); PubMed Central PMCID: PMCPMC1170174.
34. Gertler FB, Comer AR, Juang JL, Ahern SM, Clark MJ, Liebl EC, et al. Enabled, a dosage-sensitive suppressor of mutations in the *Drosophila* Abl tyrosine kinase, encodes an Abl substrate with SH3 domain-binding properties. *Genes Dev*. 1995; 9(5):521–33. PMID: [7535279](#).
35. Gertler FB, Doctor JS, Hoffmann FM. Genetic suppression of mutations in the *Drosophila* abl proto-oncogene homolog. *Science*. 1990; 248(4957):857–60. PMID: [2188361](#).
36. Comer AR, Ahern-Djamali SM, Juang JL, Jackson PD, Hoffmann FM. Phosphorylation of Enabled by the *Drosophila* Abelson tyrosine kinase regulates the in vivo function and protein-protein interactions of Enabled. *Mol Cell Biol*. 1998; 18(1):152–60. PMID: [9418863](#); PubMed Central PMCID: PMCPMC121469.
37. Kannan R, Kuzina I, Wincovitch S, Nowotarski SH, Giniger E. The Abl/enabled signaling pathway regulates Golgi architecture in *Drosophila* photoreceptor neurons. *Mol Biol Cell*. 2014; 25(19):2993–3005. <https://doi.org/10.1091/mbc.E14-02-0729> PMID: [25103244](#); PubMed Central PMCID: PMCPMC4230588.
38. Feng S, Chen JK, Yu H, Simon JA, Schreiber SL. Two binding orientations for peptides to the Src SH3 domain: development of a general model for SH3-ligand interactions. *Science*. 1994; 266(5188):1241–7. PMID: [7526465](#).

39. Yu H, Chen JK, Feng S, Dalgarno DC, Brauer AW, Schreiber SL. Structural basis for the binding of proline-rich peptides to SH3 domains. *Cell*. 1994; 76(5):933–45. PMID: [7510218](#).
40. Ren RB, Ye ZS, Baltimore D. Abl Protein-Tyrosine Kinase Selects the Crk Adapter as a Substrate Using Sh3-Binding Sites. *Gene Dev*. 1994; 8(7):783–95. <https://doi.org/10.1101/gad.8.7.783> WOS: A1994NG37600004. PMID: [7926767](#)
41. Feller SM, Knudsen B, Hanafusa H. C-Abl Kinase Regulates the Protein-Binding Activity of C-Crk. *Embo Journal*. 1994; 13(10):2341–51. WOS:A1994NM54700012. PMID: [8194526](#)
42. Riverolezcano OM, Marcilla A, Sameshima JH, Robbins KC. Wiskott-Aldrich Syndrome Protein Physiologically Associates with Nck through Src Homology-3 Domains. *Mol Cell Biol*. 1995; 15(10):5725–31. WOS:A1995RV77200056. PMID: [7565724](#)
43. Dai Z, Pendergast AM. Abi-2, a novel SH3-containing protein interacts with the c-Abl tyrosine kinase and modulates c-Abl transforming activity. *Genes Dev*. 1995; 9(21):2569–82. PMID: [7590236](#).
44. Shi Y, Alin K, Goff SP. Abl-interactor-1, a novel SH3 protein binding to the carboxy-terminal portion of the Abl protein, suppresses v-abl transforming activity. *Genes Dev*. 1995; 9(21):2583–97. PMID: [7590237](#).
45. Antoku S, Saksela K, Rivera GM, Mayer BJ. A crucial role in cell spreading for the interaction of Abl PxxP motifs with Crk and Nck adaptors. *J Cell Sci*. 2008; 121(18):3071–82. <https://doi.org/10.1242/jcs.031575> WOS:000258889400011. PMID: [18768933](#)
46. Bischof J, Maeda RK, Hediger M, Karch F, Basler K. An optimized transgenesis system for Drosophila using germ-line-specific phi C31 integrases. *Proceedings of the National Academy of Sciences of the United States of America*. 2007; 104(9):3312–7. <https://doi.org/10.1073/pnas.0611511104> WOS:000244661400053. PMID: [17360644](#)
47. Grevengoed EE, Fox DT, Gates J, Peifer M. Balancing different types of actin polymerization at distinct sites: roles for Abelson kinase and Enabled. *The Journal of cell biology*. 2003; 163(6):1267–79. <https://doi.org/10.1083/jcb.200307026> PMID: [14676307](#); PubMed Central PMCID: PMCPMC2173720.
48. Henkemeyer MJ, Gertler FB, Goodman W, Hoffmann FM. The Drosophila Abelson proto-oncogene homolog: identification of mutant alleles that have pleiotropic effects late in development. *Cell*. 1987; 51(5):821–8. PMID: [3119227](#).
49. Bennett RL, Hoffmann FM. Increased levels of the Drosophila Abelson tyrosine kinase in nerves and muscles: subcellular localization and mutant phenotypes imply a role in cell-cell interactions. *Development*. 1992; 116(4):953–66. PMID: [1295746](#).
50. Jenett A, Rubin GM, Ngo TT, Shepherd D, Murphy C, Dionne H, et al. A GAL4-driver line resource for Drosophila neurobiology. *Cell Rep*. 2012; 2(4):991–1001. <https://doi.org/10.1016/j.celrep.2012.09.011> PMID: [23063364](#); PubMed Central PMCID: PMCPMC3515021.
51. Ren R, Mayer BJ, Cicchetti P, Baltimore D. Identification of a ten-amino acid proline-rich SH3 binding site. *Science*. 1993; 259(5098):1157–61. PMID: [8438166](#).
52. Saksela K, Permi P. SH3 domain ligand binding: What's the consensus and where's the specificity? *FEBS Lett*. 2012; 586(17):2609–14. <https://doi.org/10.1016/j.febslet.2012.04.042> PMID: [22710157](#).
53. Wills Z, Bateman J, Korey CA, Comer A, Van Vactor D. The tyrosine kinase Abl and its substrate enabled collaborate with the receptor phosphatase Dlar to control motor axon guidance. *Neuron*. 1999; 22(2):301–12. PMID: [10069336](#).
54. Kidd T, Brose K, Mitchell KJ, Fetter RD, Tessier-Lavigne M, Goodman CS, et al. Roundabout controls axon crossing of the CNS midline and defines a novel subfamily of evolutionarily conserved guidance receptors. *Cell*. 1998; 92(2):205–15. PMID: [9458045](#).
55. Schultz J, Copley RR, Doerks T, Ponting CP, Bork P. SMART: a web-based tool for the study of genetically mobile domains. *Nucleic Acids Res*. 2000; 28(1):231–4. PMID: [10592234](#); PubMed Central PMCID: PMC102444.
56. Marchler-Bauer A, Bo Y, Han L, He J, Lanczycki CJ, Lu S, et al. CDD/SPARCLE: functional classification of proteins via subfamily domain architectures. *Nucleic Acids Res*. 2017; 45(D1):D200–D3. <https://doi.org/10.1093/nar/gkw1129> PMID: [27899674](#); PubMed Central PMCID: PMC5210587.
57. Drozdetskiy A, Cole C, Procter J, Barton GJ. JPred4: a protein secondary structure prediction server. *Nucleic Acids Res*. 2015; 43(W1):W389–94. <https://doi.org/10.1093/nar/gkv332> PMID: [25883141](#); PubMed Central PMCID: PMC4489285.
58. Dinkel H, Michael S, Weatheritt RJ, Davey NE, Van Roey K, Altenberg B, et al. ELM—the database of eukaryotic linear motifs. *Nucleic Acids Res*. 2012;40(Database issue):D242–51. <https://doi.org/10.1093/nar/gkr1064> PMID: [22110040](#); PubMed Central PMCID: PMC3245074.
59. Dosztanyi Z, Csizmok V, Tompa P, Simon I. IUPred: web server for the prediction of intrinsically unstructured regions of proteins based on estimated energy content. *Bioinformatics*. 2005; 21(16):3433–4. <https://doi.org/10.1093/bioinformatics/bti541> WOS:000231360600018. PMID: [15955779](#)

60. Dosztanyi Z, Csizmok V, Tompa P, Simon I. The pairwise energy content estimated from amino acid composition discriminates between folded and intrinsically unstructured proteins. *J Mol Biol.* 2005; 347(4):827–39. <https://doi.org/10.1016/j.jmb.2005.01.071> WOS:000227959200012. PMID: 15769473
61. Dosztanyi Z, Meszaros B, Simon I. ANCHOR: web server for predicting protein binding regions in disordered proteins. *Bioinformatics.* 2009; 25(20):2745–6. <https://doi.org/10.1093/bioinformatics/btp518> PMID: 19717576; PubMed Central PMCID: PMC2759549.
62. Meszaros B, Simon I, Dosztanyi Z. Prediction of Protein Binding Regions in Disordered Proteins. *PLoS computational biology.* 2009;5(5). ARTN e1000376 <https://doi.org/10.1371/journal.pcbi.1000376> WOS:000267081300021. PMID: 19412530
63. Dunker AK, Lawson JD, Brown CJ, Williams RM, Romero P, Oh JS, et al. Intrinsically disordered protein. *J Mol Graph Model.* 2001; 19(1):26–59. PMID: 11381529.
64. Song JK, Kannan R, Merdes G, Singh J, Mlodzik M, Giniger E. Disabled is a bona fide component of the Abl signaling network. *Development.* 2010; 137(21):3719–27. <https://doi.org/10.1242/dev.050948> WOS:000283669300019. PMID: 20940230
65. Nagar B, Hantschel O, Young MA, Scheffzek K, Veach D, Bornmann W, et al. Structural basis for the autoinhibition of c-Abl tyrosine kinase. *Cell.* 2003; 112(6):859–71. PMID: 12654251.
66. Patil A, Kinoshita K, Nakamura H. Domain distribution and intrinsic disorder in hubs in the human protein-protein interaction network. *Protein Sci.* 2010; 19(8):1461–8. <https://doi.org/10.1002/pro.425> PMID: 20509167; PubMed Central PMCID: PMC2923499.
67. Kim PM, Sboner A, Xia Y, Gerstein M. The role of disorder in interaction networks: a structural analysis. *Mol Syst Biol.* 2008; 4:179. <https://doi.org/10.1038/msb.2008.16> PMID: 18364713; PubMed Central PMCID: PMC2290937.
68. Babu MM, van der Lee R, de Groot NS, Gsponer J. Intrinsically disordered proteins: regulation and disease. *Curr Opin Struct Biol.* 2011; 21(3):432–40. <https://doi.org/10.1016/j.sbi.2011.03.011> PMID: 21514144.
69. Juang JL, Hoffmann FM. Drosophila Abelson interacting protein (dAbi) is a positive regulator of Abelson tyrosine kinase activity. *Oncogene.* 1999; 18(37):5138–47. <https://doi.org/10.1038/sj.onc.1202911> WOS:000082555700002. PMID: 10498863
70. Oldfield CJ, Meng J, Yang JY, Yang MQ, Uversky VN, Dunker AK. Flexible nets: disorder and induced fit in the associations of p53 and 14-3-3 with their partners. *Bmc Genomics.* 2008;9. Artn S1 <https://doi.org/10.1186/1471-2164-9-9> WOS:000206244100002.
71. Eden S, Rohatgi R, Podtelejnikov AV, Mann M, Kirschner MW. Mechanism of regulation of WAVE1-induced actin nucleation by Rac1 and Nck. *Nature.* 2002; 418(6899):790–3. <https://doi.org/10.1038/nature00859> PMID: 12181570.
72. Ibarra N, Pollitt A, Insall RH. Regulation of actin assembly by SCAR/WAVE proteins. *Biochemical Society transactions.* 2005;33(Pt 6):1243–6. <https://doi.org/10.1042/BST20051243> PMID: 16246088.
73. Shishido T, Akagi T, Chalmers A, Maeda M, Terada T, Georgescu MM, et al. Crk family adaptor proteins trans-activate c-Abl kinase. *Genes Cells.* 2001; 6(5):431–40. PMID: 11380621.
74. Reichman C, Singh K, Liu Y, Singh S, Li H, Fajardo JE, et al. Transactivation of Abl by the Crk II adapter protein requires a PNAY sequence in the Crk C-terminal SH3 domain. *Oncogene.* 2005; 24(55):8187–99. <https://doi.org/10.1038/sj.onc.1208988> WOS:000233809400010. PMID: 16158059
75. Stevens TL, Rogers EM, Koontz LM, Fox DT, Homem CCF, Nowotarski SH, et al. Using Bcr-Abl to examine mechanisms by which Abl kinase regulates morphogenesis in Drosophila. *Mol Biol Cell.* 2008; 19(1):378–93. <https://doi.org/10.1091/mbc.E07-01-0008> WOS:000258847500035. PMID: 17959833
76. Mark WY, Liao JC, Lu Y, Ayed A, Laister R, Szymczyna B, et al. Characterization of segments from the central region of BRCA1: an intrinsically disordered scaffold for multiple protein-protein and protein-DNA interactions? *J Mol Biol.* 2005; 345(2):275–87. <https://doi.org/10.1016/j.jmb.2004.10.045> PMID: 15571721.
77. Andresen C, Helander S, Lemak A, Fares C, Csizmok V, Carlsson J, et al. Transient structure and dynamics in the disordered c-Myc transactivation domain affect Bin1 binding. *Nucleic Acids Research.* 2012; 40(13):6353–66. <https://doi.org/10.1093/nar/gks263> WOS:000306970700051. PMID: 22457068
78. Mahani A, Henriksson J, Wright APH. Origins of Myc Proteins—Using Intrinsic Protein Disorder to Trace Distant Relatives. *PLoS one.* 2013;8(9). ARTN e75057 <https://doi.org/10.1371/journal.pone.0075057> WOS:000325025200020. PMID: 24086436
79. Dunker AK, Cortese MS, Romero P, Iakoucheva LM, Uversky VN. Flexible nets. The roles of intrinsic disorder in protein interaction networks. *FEBS J.* 2005; 272(20):5129–48. <https://doi.org/10.1111/j.1742-4658.2005.04948.x> PMID: 16218947.

80. Kersey PJ, Allen JE, Armean I, Boddu S, Bolt BJ, Carvalho-Silva D, et al. Ensembl Genomes 2016: more genomes, more complexity. *Nucleic Acids Res.* 2016; 44(D1):D574–80. <https://doi.org/10.1093/nar/gkv1209> PMID: 26578574; PubMed Central PMCID: PMC4702859.
81. Yates A, Akanni W, Amode MR, Barrell D, Billis K, Carvalho-Silva D, et al. Ensembl 2016. *Nucleic Acids Res.* 2016; 44(D1):D710–6. <https://doi.org/10.1093/nar/gkv1157> PMID: 26687719; PubMed Central PMCID: PMC4702834.
82. Sievers F, Wilm A, Dineen D, Gibson TJ, Karplus K, Li WZ, et al. Fast, scalable generation of high-quality protein multiple sequence alignments using Clustal Omega. *Mol Syst Biol.* 2011;7. ARTN 539 <https://doi.org/10.1038/msb.2011.75> WOS:000296652600007. PMID: 21988835
83. Goujon M, McWilliam H, Li WZ, Valentin F, Squizzato S, Paern J, et al. A new bioinformatics analysis tools framework at EMBL-EBI. *Nucleic Acids Research.* 2010; 38:W695–W9. <https://doi.org/10.1093/nar/gkq313> WOS:000284148900113. PMID: 20439314
84. Ashkenazy H, Abadi S, Martz E, Chay O, Mayrose I, Pupko T, et al. ConSurf 2016: an improved methodology to estimate and visualize evolutionary conservation in macromolecules. *Nucleic Acids Res.* 2016; 44(W1):W344–50. <https://doi.org/10.1093/nar/gkw408> PMID: 27166375; PubMed Central PMCID: PMC4987940.
85. Celniker G, Nimrod G, Ashkenazy H, Glaser F, Martz E, Mayrose I, et al. ConSurf: Using Evolutionary Data to Raise Testable Hypotheses about Protein Function. *Isr J Chem.* 2013; 53(3–4):199–206. <https://doi.org/10.1002/ijch.201200096> WOS:000317859800010.
86. Ashkenazy H, Erez E, Martz E, Pupko T, Ben-Tal N. ConSurf 2010: calculating evolutionary conservation in sequence and structure of proteins and nucleic acids. *Nucleic Acids Research.* 2010; 38:W529–W33. <https://doi.org/10.1093/nar/gkq399> WOS:000284148900085. PMID: 20478830
87. Berezin C, Glaser F, Rosenberg J, Paz I, Pupko T, Fariselli P, et al. ConSeq: the identification of functionally and structurally important residues in protein sequences. *Bioinformatics.* 2004; 20(8):1322–4. <https://doi.org/10.1093/bioinformatics/bth070> WOS:000221556100015. PMID: 14871869
88. Letunic I, Doerks T, Bork P. SMART: recent updates, new developments and status in 2015. *Nucleic Acids Research.* 2015; 43(D1):D257–D60. <https://doi.org/10.1093/nar/gku949> WOS:000350210400040. PMID: 25300481
89. Schultz J, Milpetz F, Bork P, Ponting CP. SMART, a simple modular architecture research tool: identification of signaling domains. *Proceedings of the National Academy of Sciences of the United States of America.* 1998; 95(11):5857–64. PMID: 9600884; PubMed Central PMCID: PMC4487.
90. Dosztanyi Z, Csizmok V, Tompa P, Simon I. The pairwise energy content estimated from amino acid composition discriminates between folded and intrinsically unstructured proteins. *Febs Journal.* 2005; 272:360–. WOS:000234826102046.
91. Campos-Ortega JA, Hartenstein V. Stages of Drosophila Embryogenesis. *The Embryonic Development of Drosophila melanogaster.* Berlin, Heidelberg: Springer Berlin Heidelberg; 1985. p. 9–84.
92. Schindelin J, Arganda-Carreras I, Frise E, Kaynig V, Longair M, Pietzsch T, et al. Fiji: an open-source platform for biological-image analysis. *Nat Methods.* 2012; 9(7):676–82. <https://doi.org/10.1038/nmeth.2019> PMID: 22743772; PubMed Central PMCID: PMC3855844.
93. Schindelin J, Rueden CT, Hiner MC, Eliceiri KW. The ImageJ ecosystem: An open platform for biomedical image analysis. *Mol Reprod Dev.* 2015; 82(7–8):518–29. <https://doi.org/10.1002/mrd.22489> PMID: 26153368.
94. Li CH, Tam PKS. An iterative algorithm for minimum cross entropy thresholding. *Pattern Recogn Lett.* 1998; 19(8):771–6. [https://doi.org/10.1016/S0167-8655\(98\)00057-9](https://doi.org/10.1016/S0167-8655(98)00057-9) WOS:000075193800014.
95. Hothorn T, Bretz F, Westfall P. Simultaneous inference in general parametric models. *Biom J.* 2008; 50(3):346–63. <https://doi.org/10.1002/bimj.200810425> PMID: 18481363.
96. Venables WN, Ripley BD, Venables WN. *Modern applied statistics with S.* 4th ed. New York: Springer; 2002. xi, 495 p. p.
97. Wickham H. *Ggplot2: elegant graphics for data analysis.* New York: Springer; 2009. viii, 212 p. p.
98. Fox J, Weisberg S, Fox J. *An R companion to applied regression.* 2nd ed. Thousand Oaks, Calif.: SAGE Publications; 2011. xxii, 449 p. p.
99. Hartig F. *DHARMA: Residual Diagnostics for Hierarchical (Multi-Level / Mixed) Regression Models.* <http://florianhartig.github.io/DHARMA/2017>.
100. Cameron AC, Trivedi PK. Regression-Based Tests for Overdispersion in the Poisson Model. *J Econometrics.* 1990; 46(3):347–64. [https://doi.org/10.1016/0304-4076\(90\)90014-K](https://doi.org/10.1016/0304-4076(90)90014-K) WOS: A1990EL35200005.
101. Cameron AC, Trivedi PK. *Regression analysis of count data.* Cambridge, UK; New York, NY, USA: Cambridge University Press; 1998. xvii, 411 p. p.

102. Cameron AC, Trivedi PK. *Microeconometrics: methods and applications*. Cambridge; New York: Cambridge University Press; 2005. xxii, 1034 p. p.
103. Bartlett MS. Properties of sufficiency and statistical tests. *Proc R Soc Lon Ser-A*. 1937; 160 (A901):0268–82. <https://doi.org/10.1098/rspa.1937.0109> WOS:000200958100009.
104. Taagepera S, McDonald D, Loeb JE, Whitaker LL, McElroy AK, Wang JY, et al. Nuclear-cytoplasmic shuttling of C-ABL tyrosine kinase. *Proceedings of the National Academy of Sciences of the United States of America*. 1998; 95(13):7457–62. PMID: [9636171](https://pubmed.ncbi.nlm.nih.gov/9636171/); PubMed Central PMCID: PMCPMC22649.
105. Wen ST, Jackson PK, Van Etten RA. The cytostatic function of c-Abl is controlled by multiple nuclear localization signals and requires the p53 and Rb tumor suppressor gene products. *EMBO J*. 1996; 15 (7):1583–95. PMID: [8612582](https://pubmed.ncbi.nlm.nih.gov/8612582/); PubMed Central PMCID: PMCPMC450068.
106. Miao YJ, Wang JY. Binding of A/T-rich DNA by three high mobility group-like domains in c-Abl tyrosine kinase. *The Journal of biological chemistry*. 1996; 271(37):22823–30. PMID: [8798460](https://pubmed.ncbi.nlm.nih.gov/8798460/).
107. Miller AL, Wang Y, Mooseker MS, Koleske AJ. The Abl-related gene (Arg) requires its F-actin-microtubule cross-linking activity to regulate lamellipodial dynamics during fibroblast adhesion. *The Journal of cell biology*. 2004; 165(3):407–19. <https://doi.org/10.1083/jcb.200308055> PMID: [15138293](https://pubmed.ncbi.nlm.nih.gov/15138293/); PubMed Central PMCID: PMCPMC2172189.
108. Wang Y, Miller AL, Mooseker MS, Koleske AJ. The Abl-related gene (Arg) nonreceptor tyrosine kinase uses two F-actin-binding domains to bundle F-actin. *Proceedings of the National Academy of Sciences of the United States of America*. 2001; 98(26):14865–70. <https://doi.org/10.1073/pnas.251249298> PMID: [11752434](https://pubmed.ncbi.nlm.nih.gov/11752434/); PubMed Central PMCID: PMCPMC64950.